

RADBOD UNIVERSITY NIJMEGEN



FACULTY OF SCIENCE

---

# Power Grid Failures

*Theory of Fluctuating Renewables*

---

THESIS BSc MATHEMATICS

*Author:*

Fons VAN DER PLAS

*Supervisor:*

dr. Henk DON

*Second reader:*

prof. dr. Eric CATOR

June 2019

# Notation

$\mathbf{Y}$  is a matrix or vector

$Y_{i,j}$  is an element of a matrix or vector

$Y$  is a (real or complex) number

$Y$  is a physical quantity (like ‘admittance’)

$[n] = \{1, \dots, n\}$

Een geel doosje geeft aan dat een stuk tekst *nog geschreven moet worden*.

Een oranje doosje is meer *voor mezelf*, dingen waar ik later nog naar moet kijken.

Een groen doosje geeft *bronnen* aan die relevant (kunnen) zijn.

# Contents

<b>I</b>	<b>Theory of Electric Power Networks</b>	<b>4</b>
<b>1</b>	<b>Probability Theory</b>	<b>5</b>
1.1	*Abstract Integration . . . . .	5
1.2	*Probability Measure . . . . .	5
1.3	Large Deviation Theory . . . . .	5
1.4	Multivariate Gaussian distribution . . . . .	5
<b>2</b>	<b>Graph theory</b>	<b>12</b>
2.1	Directed graphs . . . . .	12
2.2	Flow . . . . .	12
<b>3</b>	<b>Circuit Theory</b>	<b>18</b>
3.1	*DC Circuits . . . . .	18
3.2	AC Circuits . . . . .	18
<b>4</b>	<b>The Electric Grid</b>	<b>19</b>
4.1	Overview . . . . .	19
4.2	Generators . . . . .	20
4.3	Loads . . . . .	20
4.4	Transmission . . . . .	21
4.5	Power Flow Analysis . . . . .	23
4.6	Transmission grid operation . . . . .	23
<b>5</b>	<b>Modelling Transmission Networks</b>	<b>29</b>
5.1	Grid structure . . . . .	30
5.2	Power grid state . . . . .	32
5.3	State validity . . . . .	32

5.4	Power Flow . . . . .	38
5.5	DC approximation . . . . .	38
5.6	Linear Power Flow . . . . .	44
5.7	Stochastic power injections . . . . .	45
5.8	Redistribution of flow . . . . .	47
<b>II</b>	<b>Predicting failures in Germany's grid</b>	<b>52</b>
<b>6</b>	<b>Methods</b>	<b>53</b>
6.1	Constructing a complete dataset . . . . .	54
6.2	LPF . . . . .	56
6.3	Stochastic power injection . . . . .	56
6.4	Line failures . . . . .	57
6.5	Cascading line failures . . . . .	57
<b>7</b>	<b>Results</b>	<b>58</b>
7.1	SciGRID data . . . . .	58
7.2	Bus covariance . . . . .	60
7.3	Line covariance . . . . .	60

## **Part I**

# **Theory of Electric Power Networks**

## Chapter one

# Probability Theory

### 1.1 \*Abstract Integration

Lebesgue-Stieltjes integral

### 1.2 \*Probability Measure

Should cover: p. measure, cont. distr., stochastic vectors, E, moment gen?, CLT, multivar norm dist

See Rynne or Garling or Analyse de Hilbert et de Fourier course notes

See Pestman or MIT course notes or...

### 1.3 Large Deviation Theory

Should cover: application to multivariate normal dist

See Hugo or MIT course notes or ...

### 1.4 Multivariate Gaussian distribution

*This presentation of the multivariate Gaussian distribution is heavily based on Chapter VIII of Mathematical Statistics by Pestman (1998), which provides proofs to all theorems listed below.*

One distribution that will be particularly useful in our analysis is the *multivariate Gaussian distribution*, which generalised the (one-dimensional) normal distribution. In the simplest case, we have a stochastic vector  $\mathbf{E} = (E_1, \dots, E_p)$ , which is the combination of  $p$  normally distributed, *independent* scalar variables. In general, however, we wish to study stochastic vectors produced by applying a *linear transformation*  $\mathbf{L} \in \mathcal{L}(\mathbb{R}^p, \mathbb{R}^q)$  to  $\mathbf{E}$ . In this case, the coordinate variables  $(\mathbf{L}\mathbf{E})_1, \dots, (\mathbf{L}\mathbf{E})_q$  are not always independent!

For example, the map  $(E_1, E_2) \mapsto (E_1, E_1 + E_2)$  transforms two independent normals into two dependent ones.

Deze inleiding slaat het geval  $E$  Gaussiaans maar niet normaal, over.

### 1.4.1 Normal and Gaussian

Although they are often used interchangeably, we make a clear distinction between a *normal* distribution and a *Gaussian* distribution. The former should be familiar:

**Definition 1.4.1.** A scalar variable  $E$  is said to be *normally distributed* with parameters  $\mu$  and  $\sigma$  if

$$x \mapsto \frac{1}{\sigma\sqrt{2\pi}} \exp \left[ \frac{-(x - \mu)^2}{2\sigma^2} \right] \quad (1.1)$$

is the probability density of  $E$ .

**Definition 1.4.2.** A scalar variable  $E$  is said to be *Gaussian distributed* if it is either normally distributed or constant.

One could interpret a constant  $E$  with value  $\mu$  as a normally distributed variable with mean  $\mu$  and ‘standard deviation 0’. Clearly, a linear combination of Gaussian distributed scalar variables is also Gaussian distributed.

**Definition 1.4.3.** A stochastic vector  $\mathbf{E} = (E_1, \dots, E_p)$  is *elementary normally distributed* if the scalar variables  $E_i$  are independent and normally distributed ( $i \in [p]$ ).  $\mathbf{E}$  is *elementary Gaussian distributed* if the scalar variables  $E_i$  are independent and Gaussian distributed.

**Definition 1.4.4.** A stochastic vector  $\mathbf{X} = (X_1, \dots, X_p)$  is *normally distributed* if there exists an orthogonal operator  $\mathbf{Q}$  such that  $\mathbf{QX}$  is elementary normally distributed.  $\mathbf{X}$  is *Gaussian distributed* if there exists an orthogonal operator  $\mathbf{Q}$  such that  $\mathbf{QX}$  is elementary normally distributed.

Plaatjes vullen gaatjes

We state, without proof, the following properties of Gaussian distributed vectors:

**Proposition 1.4.5.** *The distribution of a Gaussian distributed vector  $\mathbf{X}$  is uniquely determined by its expectation  $\boldsymbol{\mu} = \mathbb{E}[\mathbf{X}]$  and covariance matrix  $\boldsymbol{\Sigma} = \mathcal{C}(\mathbf{X})$ , and we write  $\mathbf{X} \sim \mathcal{N}(\boldsymbol{\mu}, \boldsymbol{\Sigma})$ .  $\mathbf{X}$  is normally distributed if and only if  $\boldsymbol{\Sigma}$  is invertible.*

define cov-mat

Translating or applying a linear map to a Gaussian distribution results in a new Gaussian distribution. Note that this can be *any* linear map, not necessarily a bijective, orthogonal one.

**Theorem 1.4.6.** *Suppose  $\mathbf{X}$  is a  $\mathcal{N}(\boldsymbol{\mu}, \boldsymbol{\Sigma})$ -distributed  $p$ -vector.*

For any  $\mathbf{a} \in \mathbb{R}^p$ :

$$\mathbf{X} + \mathbf{a} \sim \mathcal{N}(\boldsymbol{\mu} + \mathbf{a}, \boldsymbol{\Sigma}), \quad (1.2)$$

and for any linear map  $\mathbf{L} \in \mathcal{L}(\mathbb{R}^p, \mathbb{R}^q)$ :

$$\mathbf{L}\mathbf{X} \sim \mathcal{N}(\mathbf{L}\boldsymbol{\mu}, \mathbf{L}\boldsymbol{\Sigma}\mathbf{L}^*). \quad (1.3)$$

**Corollary 1.4.6.1.** For any  $\mathbf{b} \in \mathbb{R}^p$ , the mapping

$$\mathbf{b}^* : \mathbb{R}^p \rightarrow \mathbb{R} : \mathbf{x} \mapsto \langle \mathbf{x}, \mathbf{b} \rangle$$

is linear, and therefore the scalar variable  $\mathbf{b}^*\mathbf{X} = \langle \mathbf{X}, \mathbf{b} \rangle$  is Gaussian distributed.

In particular, when applying Corollary 1.4.6.1 to each element of the standard basis  $(\mathbf{e}_1, \dots, \mathbf{e}_p)$  of  $\mathbb{R}^p$ , we find that each of the *coordinates* of  $\mathbf{X}$  is Gaussian distributed:

**Proposition 1.4.7.** Suppose  $\mathbf{X} = (X_1, \dots, X_p)$  is a  $\mathcal{N}(\boldsymbol{\mu}, \boldsymbol{\Sigma})$ -distributed  $p$ -vector. Then each for each  $i \in [p]$ , the marginal distribution is given by:

$$X_i \sim \mathcal{N}(\mu_i, \Sigma_{ii}).$$

For normal distributed vectors, a probability density function exists:

**Theorem 1.4.8.** Suppose  $\mathbf{X}$  is a normally distributed  $p$ -vector with expectation  $\boldsymbol{\mu} = \mathbb{E}[\mathbf{X}]$  and covariance matrix  $\boldsymbol{\Sigma} = \mathcal{C}(\mathbf{X})$ . Then  $\mathbf{X}$  has a probability density function given by

$$\mathbf{x} \mapsto \frac{1}{\sqrt{\det(\boldsymbol{\Sigma})} (2\pi)^{p/2}} \exp \left[ -\frac{1}{2}(\mathbf{x} - \boldsymbol{\mu})^* \boldsymbol{\Sigma}^{-1}(\mathbf{x} - \boldsymbol{\mu}) \right] \quad (1.4)$$

*Remark.* The condition that  $\mathbf{X}$  is normally distributed is necessary: if  $\mathbf{X}$  is Gaussian, but not normal, it will take values in an *affine subspace* of  $\mathbb{R}^p$  (such as a plane, as subspace of  $\mathbb{R}^3$ ). If a density function were to exist, it would have support of zero measure, and integrating over  $\mathbb{R}^p$  would yield 0, instead of 1.

**Theorem 1.4.9.** The mode of a Gaussian distribution is its mean.

## 1.4.2 One linear condition

**Definition 1.4.10.** Given a  $\mathbf{r} \in \mathbb{R}^p$  and  $b \in \mathbb{R}$ , the set  $A \subseteq \mathbb{R}^p$  of solutions to the equation

$$\langle \mathbf{r}, \mathbf{x} \rangle = b$$

is called a *plane* in  $\mathbb{R}^p$ . The set  $B \subseteq \mathbb{R}^p$  of solutions to

$$\langle \mathbf{r}, \mathbf{x} \rangle \leq b$$

is a *half-space* in  $\mathbb{R}^p$ . When  $b = 1$ , we write  $\mathbf{r}_A$ , and we say that  $\mathbf{r}_A$  is a *pillar* for  $A$ . Two planes are called *parallel* if they do not intersect.

*Remark.* When  $b \neq 1$ , we can scale  $\mathbf{r}$  to create a pillar for  $A$  or  $B$ , unless  $b = 0$  (which is the case if and only if  $\mathbf{0} \in A, B$ , respectively).

*Remark.*  $A = \partial B$ .

Orthogonal projection onto a plane

positive def-  
inite keer  
normaal is  
normaal

Klopt dit?

(waar) moet  
dit?



**Definition 1.4.11.** A *convex polyhedron* in  $\mathbb{R}^p$  is the intersection of finitely many half-spaces in  $\mathbb{R}^p$ , and can be written as the set of solutions to

$$\mathbf{R}\mathbf{x} \leq \mathbf{b},$$

where each  $i$ th row of  $\mathbf{R}$ , together with  $b_i$ , defines one of the intersecting half-spaces.

The boundary of a convex polyhedron is contained in the union of planes corresponding to the half-spaces. This relation is strict, in general.

The convex polyhedra in  $\mathbb{R}$  are exactly all (possibly infinite) closed intervals. Convex polyhedra in  $\mathbb{R}^3$  are familiar shapes, like a cube or a pyramid, but they might also be unbounded, like a pyramid with infinitely deep foundations. Objects that are *not* convex polyhedra are spheres (no finite intersection of half-spaces) and donuts (not convex, which as the name suggest, is a property of any convex polyhedron<sup>1</sup>).

In this thesis, we model the *power injection* of a grid as a normally distributed stochastic vector, where each coordinate corresponds to the amount of energy injected at a node of the network. Positive values denote net generation (injection) and negative values are assigned to net consumption. The stochastic behaviour originates from *renewable sources*: wind and solar, and their correlations arise from correlated weather.

The transmission network was built to transfer power from one node to another, i.e. have a non-zero power injection. In Chapter 4, we will learn that not all power injections are *feasible*, as some might cause one of the transmission lines to overload. The *feasibility region* (the set of power injections that can be used) is, to some approximation, a *convex polyhedron*.

Using historical generation series, we can estimate the covariance of this power injection. Because the amount of current flowing through a line is a linear function of the power injection (by the same approximation), we can use Corollary 1.4.6.1 to determine the marginal distribution of line current, which gives the probability of an overload failure. A failure of this kind (i.e. caused by a fluctuation of renewable injection) is called an *emergent failure*.

Current studies (notably Nesti et al. (2018a) and Chertkov et al. (2011)) take this one step further, by determining *the most probable power injection that caused the emergent failure to occur*. We follow the approach of Nesti et al. (2018a), which is generalised in the following Theorem. Here, the plane  $A$  can be taken to be one of the *boundary planes of the feasibility region, corresponding to one of the lines*, and the event  $\mathbf{X} \in A$  is the *moment that this line overloads*.

**Theorem 1.4.12.** Let  $\mathbf{X} \sim \mathcal{N}(\boldsymbol{\mu}, \boldsymbol{\Sigma})$  be a normally distributed  $p$ -vector with density function  $f_{\mathbf{X}}$ , and let  $A \subseteq \mathbb{R}^p$  be a plane, given by a pillar  $\mathbf{r}_A \in \mathbb{R}^p$ . Then  $\mathbf{X} \mid A$  is Gaussian distributed, and has mode

$$\tilde{\mathbf{x}}_A = \operatorname{argmax}_{\mathbf{x} \in A} f_{\mathbf{X}}(\mathbf{x}) = \boldsymbol{\mu} + \frac{1 - \langle \boldsymbol{\mu}, \mathbf{r}_A \rangle}{\langle \boldsymbol{\Sigma} \mathbf{r}_A, \mathbf{r}_A \rangle} \boldsymbol{\Sigma} \mathbf{r}_A. \quad (1.5)$$

*Proof.* We will start with the special case of  $\boldsymbol{\Sigma} = \mathbf{I}$ , and work our way towards the general case.<sup>2</sup>

<sup>1</sup>Using the linearity of the inner product, one easily finds that half-spaces are convex, and so are their intersections.

<sup>2</sup>This process uses the so-called the *standardised form* of  $\mathbf{X}$ .

hier bestaat vast notatie voor

$A$  is not an event, but  $\mathbf{X}^{-1}(A)$  is.

inproduct  $\mathbf{r}\mathbf{x}$  is verkeerd om

*Step 1. The case of unit covariance.*

Suppose  $\mathbf{X}$  is *elementary* normally distributed, with all marginal variances equal to one, i.e.  $\Sigma = \Sigma^{-1} = \mathbf{I}$ . The probability density function of  $X$  (see Equation (1.4)) then reduces to:

$$\mathbf{x} \mapsto \frac{1}{(2\pi)^{p/2}} \exp \left[ -\frac{\|\mathbf{x} - \boldsymbol{\mu}\|^2}{2} \right].$$

This is a *decreasing* function of the *distance between  $\mathbf{x}$  and  $\boldsymbol{\mu}$* , and so its mode is obtained when this distance is minimum.

Because  $A$  is an affine subspace of  $\mathbb{R}^p$ , the distance between  $\mathbf{x} \in A$  and  $\boldsymbol{\mu}$  is minimum when  $\mathbf{x}$  is the *orthogonal projection* of  $\boldsymbol{\mu}$  onto  $A$ , which is given by:

$$\tilde{\mathbf{x}}_A = \boldsymbol{\mu} + \frac{1 - \langle \boldsymbol{\mu}, \mathbf{r}_A \rangle}{\langle \mathbf{r}_A, \mathbf{r}_A \rangle} \mathbf{r}_A.$$

*Step 2. The case of an arbitrary elementary normal distribution.*

Let us drop the assumption that all marginal variances are equal to one. There exist  $\lambda_1, \dots, \lambda_p \in \mathbb{R}_{>0}$  such that  $\Sigma = \Lambda = \text{diag}(\lambda_1, \dots, \lambda_p)$ , and  $\Lambda^t = \text{diag}(\lambda_1^t, \dots, \lambda_p^t)$  for any  $t \in \mathbb{R}$ . With  $t = -\frac{1}{2}$ , we find that  $\Lambda^{-\frac{1}{2}}\mathbf{X}$  is elementary normally distributed, with mean  $\Lambda^{-\frac{1}{2}}\boldsymbol{\mu}$  and unit covariance matrix. Applying the same transformation  $\Lambda^{-\frac{1}{2}}$  to  $A$  yields a new plane, which has pillar  $\Lambda^{\frac{1}{2}}\mathbf{r}_A$  (not  $\Lambda^{-\frac{1}{2}}\mathbf{r}_A$ ):

For each  $\mathbf{x} \in \mathbb{R}^p$ , we have

$$\mathbf{x} \in A \iff$$

$$\begin{aligned} \langle \mathbf{x}, \mathbf{r}_A \rangle = 1 &\iff \sum_{i=1}^p x_i r_{A,i} = 1 \iff \sum_{i=1}^p \lambda_i^{-\frac{1}{2}} x_i \lambda_i^{\frac{1}{2}} r_{A,i} = 1 \iff \\ &\langle \Lambda^{-\frac{1}{2}} \mathbf{x}, \Lambda^{\frac{1}{2}} \mathbf{r}_A \rangle = 1 \iff \langle \Lambda^{-\frac{1}{2}} \mathbf{x}, \mathbf{r}_{\Lambda^{-\frac{1}{2}}(A)} \rangle = 1 \\ &\iff \Lambda^{-\frac{1}{2}} \mathbf{x} \in \Lambda^{-\frac{1}{2}}(A). \end{aligned}$$

This means that the plane  $\Lambda^{-\frac{1}{2}}(A)$  is defined by the pillar  $\Lambda^{\frac{1}{2}}\mathbf{r}_A$ .

We can now apply our earlier result, and we find:

$$\begin{aligned} \tilde{\mathbf{x}}_A &= \Lambda^{\frac{1}{2}} \left( \overline{\Lambda^{-\frac{1}{2}} \mathbf{x}}_{\Lambda^{-\frac{1}{2}}(A)} \right) = \Lambda^{\frac{1}{2}} \left( \Lambda^{-\frac{1}{2}} \boldsymbol{\mu} + \frac{1 - \langle \Lambda^{-\frac{1}{2}} \boldsymbol{\mu}, \Lambda^{\frac{1}{2}} \mathbf{r}_A \rangle}{\langle \Lambda^{\frac{1}{2}} \mathbf{r}_A, \Lambda^{\frac{1}{2}} \mathbf{r}_A \rangle} \Lambda^{\frac{1}{2}} \mathbf{r}_A \right) \\ &= \boldsymbol{\mu} + \frac{1 - \langle \Lambda^{-\frac{1}{2}} \boldsymbol{\mu}, \Lambda^{\frac{1}{2}} \mathbf{r}_A \rangle}{\langle \Lambda^{\frac{1}{2}} \mathbf{r}_A, \Lambda^{\frac{1}{2}} \mathbf{r}_A \rangle} \Lambda \mathbf{r}_A = \boldsymbol{\mu} + \frac{1 - \langle \boldsymbol{\mu}, \mathbf{r}_A \rangle}{\langle \Lambda \mathbf{r}_A, \mathbf{r}_A \rangle} \Lambda \mathbf{r}_A. \end{aligned}$$

*Step 3. The general case.*

Finally, we consider the general case where  $\mathbf{X}$  is normally distributed. If so, there exists orthogonal  $\mathbf{Q}$  such that  $\Sigma = \mathbf{Q}\Lambda\mathbf{Q}^{-1}$ , with  $\Lambda$  a diagonal matrix. In other words, the orthogonal map  $\mathbf{Q}^{-1}$  maps  $\mathbf{X}$  into an *elementary* normally distributed vector.<sup>3</sup> Applying the same transformation  $\mathbf{Q}^{-1}$  to  $A$  yields a new plane, which is defined by the pillar  $\mathbf{Q}^{-1}\mathbf{r}_A$ . This derivation is more straightforward, since  $\mathbf{Q}^{-1}$  is orthogonal:

<sup>3</sup> $\mathbf{Q}^{-1}\mathbf{X}$  is elementary normally distributed, but it does not necessarily have a unit covariance matrix.

Dit zijn  
e vari-  
anties, ge-  
bruikt sim-  
gasquared?

For each  $\mathbf{x} \in \mathbb{R}^p$ , we have

$$\mathbf{x} \in A \iff$$

$$\begin{aligned} \langle \mathbf{x}, \mathbf{r}_A \rangle = 1 &\iff \langle \mathbf{Q}^{-1}\mathbf{x}, \mathbf{Q}^{-1}\mathbf{r}_A \rangle = 1 \iff \langle \mathbf{Q}^{-1}\mathbf{x}, \mathbf{r}_{\mathbf{Q}^{-1}(A)} \rangle = 1 \\ &\iff \mathbf{Q}^{-1}\mathbf{x} \in \mathbf{Q}^{-1}(A). \end{aligned}$$

Using our previous result, we find:

$$\begin{aligned} \tilde{\mathbf{x}}_A &= \mathbf{Q} \left( \overline{(\mathbf{Q}^{-1}\mathbf{x})_{\mathbf{Q}^{-1}(A)}} \right) = \mathbf{Q} \left( \mathbf{Q}^{-1}\boldsymbol{\mu} + \frac{1 - \langle \mathbf{Q}^{-1}\boldsymbol{\mu}, \mathbf{Q}^{-1}\mathbf{r}_A \rangle}{\langle \Lambda \mathbf{Q}^{-1}\mathbf{r}_A, \mathbf{Q}^{-1}\mathbf{r}_A \rangle} \Lambda \mathbf{Q}^{-1}\mathbf{r}_A \right) \\ &= \boldsymbol{\mu} + \frac{1 - \langle \mathbf{Q}^{-1}\boldsymbol{\mu}, \mathbf{Q}^{-1}\mathbf{r}_A \rangle}{\langle \Lambda \mathbf{Q}^{-1}\mathbf{r}_A, \mathbf{Q}^{-1}\mathbf{r}_A \rangle} \mathbf{Q} \Lambda \mathbf{Q}^{-1}\mathbf{r}_A = \boldsymbol{\mu} + \frac{1 - \langle \boldsymbol{\mu}, \mathbf{r}_A \rangle}{\langle \mathbf{Q} \Lambda \mathbf{Q}^{-1}\mathbf{r}_A, \mathbf{r}_A \rangle} \mathbf{Q} \Lambda \mathbf{Q}^{-1}\mathbf{r}_A \\ &= \boldsymbol{\mu} + \frac{1 - \langle \boldsymbol{\mu}, \mathbf{r}_A \rangle}{\langle \boldsymbol{\Sigma} \mathbf{r}_A, \mathbf{r}_A \rangle} \boldsymbol{\Sigma} \mathbf{r}_A. \end{aligned}$$



When we replace the *plane*  $A$  by a *half-space*  $B$  in Theorem 1.4.12, there are two cases to consider. If  $\boldsymbol{\mu} \in B$ , then  $\tilde{\mathbf{x}}_B = \boldsymbol{\mu}$ , because the mode of  $\mathbf{X}$  is  $\boldsymbol{\mu}$ , which is contained in  $B$ .

In the non-trivial case of  $\boldsymbol{\mu} \notin B$ , we find that  $\tilde{\mathbf{x}}_B = \tilde{\mathbf{x}}_A$ , where  $A := \partial B$  is the *boundary* of  $B$ , which is a plane, given by the same pillar:  $\mathbf{r}_A = \mathbf{r}_B$ . A geometrical argument is as follows: by reducing to the case of an elementary normally distributed  $\mathbf{X}$  with a unit covariance matrix, the mode is the point of  $B$  that minimises the distance to  $\boldsymbol{\mu}$ . Since  $\boldsymbol{\mu} \notin B$ , this point must lie on the boundary of  $B$ , i.e.  $\tilde{\mathbf{x}}_B \in A$ . Because  $A$  is a subset of  $B$ , we can proceed to compute  $\tilde{\mathbf{x}}_A$ , which is then necessarily the mode of  $\mathbf{X} \mid B$ .

For a half-plane  $B$ , we now have an explicit expression for  $\tilde{\mathbf{x}}_B$ , i.e. the *most likely value* of  $\mathbf{X}$ , given that  $\mathbf{X} \in B$ . What can we say about the *expected value* of  $\mathbf{X} \mid B$ ? Geometrically, one can imagine that  $\mathbb{E}[\mathbf{X} \mid \mathbf{X} \in B]$  lies close to  $\tilde{\mathbf{x}}_B$ , but ‘shifted inwards’, away from  $\partial B$  (in the direction of its pillar). We have not found a direct method to compute this expected value. Nesti et al. (2018a) introduce a scaling factor  $\epsilon > 0$  to the covariance of  $\mathbf{X}$  (i.e.  $\mathbf{X}_\epsilon \sim \mathcal{N}(\boldsymbol{\mu}, \epsilon \boldsymbol{\Sigma})$ ), and show that the expected value *converges* to  $\tilde{\mathbf{x}}_B$ , the mode,<sup>4</sup> as  $\epsilon \rightarrow 0$ , using the tools of Large Deviations Theory.

One can interpret this result as saying that the probability density of  $\mathbf{X}_\epsilon \mid B$  gets *concentrated close to the boundary* of  $B$ . In the one-dimensional case, this statement<sup>5</sup> is easy to demonstrate, see e.g. Touchette (2009).

Is de marginale verdeling gaussiaans verdeeld? (Ze is niet normaal verdeeld.) Wat is de covariantiematrix? Je zou als Stap 0 kunnen transformeren naar een  $\mathbf{r}_A$  die parallel aan een van de assen loopt, en dan dat coördinaat gelijk aan  $\|\mathbf{r}_A\|$  stellen? Maar dan klopt de verwachtingswaarde niet meer?

<sup>4</sup>The factor  $\epsilon$  disappears in (1.5).

<sup>5</sup>i.e. the *tail distribution* of  $X \sim \mathcal{N}(0, \epsilon^2)$ , given  $X \geq 1$ , becomes *steeper* as  $\epsilon \rightarrow 0$ .

Het zou mooier zijn om dit resultaat toe te passen op een algemene Gauss-verdeling, die niet per se normaal is. De marginale verdeling bestaat dan alleen niet altijd, namelijk wanneer  $A \cap \text{Im}(\mathbf{X}) = \emptyset$ . Als ze wel bestaat, dan gok ik dat het Gaussiaans is.

Het is nu niet toe te passen op line flows (want die zijn normaal, wel Gaussiaans), maar wel op de injectie. Wanneer je dan de meest likely injectie hebt, kan je afleiden wat de flow is. Dit komt overeen met elkaar?

De covariantiematrix van de flow is ook bijna singulair (numeriek gezien singulair), omdat de correlaties zo sterk zijn. Maar ik denk dat je kan beargumenteren dat de kans op singuliere covariantiematrix 0 is, en dan kan de stelling dus wel worden toegepast. Numeriek is de bijna-singulariteit ook geen probleem (denk ik), omdat in de uiteindelijke uitdrukking de inverse van sigma niet voorkomt.

## Chapter two

# Graph theory

## 2.1 Directed graphs

When studying the flow of current in a network, it is useful to fix a direction for each line, relative to which the flow can be expressed. Semantically, a *positive* flow along an edge will mean a flow in the same direction as the edge, while a *negative* flow describes a 'positive' flow in the opposite direction. The choice of line direction could be seen as arbitrary.

**Definition 2.1.1.** A *directed graph* is a pair  $(\mathcal{N}, \mathcal{L})$  such that the set of *nodes*  $\mathcal{N}$  is finite, and the set of *lines*  $\mathcal{L} \subseteq \mathcal{N} \times \mathcal{N}$  satisfies:

- If  $(i, j) \in \mathcal{L}$ , then  $(j, i) \notin \mathcal{L}$ . (i.e. there are no 'loops' between two nodes.)
- For each  $i \in \mathcal{N}$ :  $(i, i) \notin \mathcal{L}$ . (i.e. no node is directly connected to itself.)

*Remark.* Note that the second requirement follows from the first.

undirected graph, subgraph, path, loop, euler path, connected, k-edge-connectivity, tree, minimum spanning subtree

thm: every connected graph contains a spanning subtree

thm:  $G$  is a tree iff  $m=n-1$

thm: removing a leaf from a tree results in a new tree

thm: eulerian path in een boom is uniek

If including maxwell derivation: graph topology, calculus on graphs

When flow is complex-valued, there is no pos/neg.

It turns out that this concept is called a 'Gain Graph' (wiki)

## 2.2 Flow

intro

For the remainder of this section, assume that  $G = (\mathcal{N}, \mathcal{L})$  is a directed graph, where the nodes are labelled  $\mathcal{N} = \{1, 2, \dots, n\} = [n]$  for some  $n \in \mathbb{N}$ .

The  $m = \#\mathcal{L}$  lines of the network are labelled  $\mathcal{L} = \{\mathcal{L}_1, \mathcal{L}_2, \dots, \mathcal{L}_m\}$ .

Suppose  $\mathbb{K}$  is a field.

**Definition 2.2.1.** An *injection* is an element of  $\mathbb{K}^n$ .

**Definition 2.2.2.** A *flow* is an element of  $\mathbb{K}^m$ .

semantics

When  $\mathbb{K} = \mathbb{F}_2$ , a flow can be seen as a subset of the collection of lines  $\mathcal{L}$

**Definition 2.2.3.** An injection  $\mathbf{p} \in \mathbb{K}^n$  is *induced* by a flow  $\mathbf{f} \in \mathbb{K}^m$  if:

$$p_i = \sum_{\mathcal{L}_k=(i,j) \in \mathcal{L}} f_k - \sum_{\mathcal{L}_k=(j,i) \in \mathcal{L}} f_k \quad (2.1)$$

for each node  $i \in \mathcal{N}$ .

Note that  $\mathbf{p}$  is uniquely defined for every choice of  $\mathbf{f}$ , under the condition that  $G$  has no *isolated nodes*: nodes with no lines connecting them. This allows us to define a function:

not necessary

**Definition 2.2.4.** Suppose  $G$  has no isolated nodes. We define the *Flow Response Transformation* (FRT) as the function

$$\text{FRT} : \mathbb{K}^m \rightarrow \mathbb{K}^n$$

which maps a flow  $\mathbf{f} \in \mathbb{K}^m$  to the unique injection  $\mathbf{p} \in \mathbb{K}^n$  that it induces.

From (2.1), it follows that FRT is a linear map. In fact, when written in matrix form, we find a familiar result: the transposed edge-vertex incidence matrix of  $G$ !

blub

$$\text{FRT} = \mathbf{C}^T$$

The fact that FRT is a linear map raises an interesting question: how can the image and kernel of FRT be interpreted in the context of digraph flows? The reader is invited to revisit [Example](#) to visualise these sets.

examples

One can interpret the image of FRT as the set of injections that can be redistributed along the network. Because a flow only serves to redistribute injections from one node to another, nothing is lost or gained in the network. This imposes the condition that an injection vector must have *zero sum*. Moreover, when  $G$  is connected, *all* zero sum injections can be induced by a flow.

The kernel can be interpreted as the set of all flows that result in zero injections. Besides the trivial case of zero flow, any constant flow along a closed loop induces zero injection. We will find that these *loop flows* generate *all* flows in the kernel of FRT.

When  $G$  is a planar graph, loops around the faces of  $G$  actually form a *basis* for the kernel. In the more general case that  $G$  is connected, but not necessarily planar, such a basis can also be constructed by fixing a *spanning subtree* of  $G$ .

As an added bonus, applying the Rank-Nullity theorem to FRT when  $G$  is planar provides us with an alternative proof of Euler's Formula.

These statements will be made more precise in the next sections, when we study the image and kernel of FRT in more detail.

### 2.2.1 Image of FRT

intro

**Definition 2.2.5.** The function  $\sigma : \mathbb{K}^n \rightarrow \mathbb{K}$  defined by

$$\sigma : \mathbf{p} \mapsto \sum_{i=1}^n p_i$$

is the linear map from an injection vector  $\mathbf{p}$  to the *net injection* of  $\mathbf{p}$ .

The kernel of  $\sigma$  is the set of zero-sum injections:

$$\ker \sigma = \left\{ \mathbf{p} \in \mathbb{K}^n \mid \sum_{i=1}^n p_i = 0 \right\}.$$

When  $G$  is connected, this is exactly the set of injections that can be induced by a flow on  $G$ :

**Theorem 2.2.6.** *Suppose that  $G$  is connected. Then*


$$\text{Im FRT} = \left\{ \mathbf{p} \in \mathbb{K}^n \mid \sum_{i=1}^n p_i = 0 \right\} \cong \mathbb{K}^{n-1} \quad (2.2)$$

We will prove this equality by considering the two inclusions  $\subseteq$  and  $\supseteq$  separately. The first inclusion follows from the observation that  $\text{FRT} = \mathbf{C}^T$ :

**Lemma 2.2.7.** *Suppose that  $G$  is connected.*

$$\text{Im FRT} \subseteq \ker \sigma \quad (2.3)$$

*Proof.* We write  $\mathbf{e}^1, \dots, \mathbf{e}^m$  for the standard basis of  $\mathbb{K}^m$ .

Since FRT is linear, one only needs to verify that  $\text{FRT}(\mathbf{f}) \in \ker \sigma$  for each  $\mathbf{f} = \mathbf{e}^k$  in the basis. The vectors  $\text{FRT}(\mathbf{e}^1), \dots, \text{FRT}(\mathbf{e}^m)$  are exactly the columns of the matrix  $\text{FRT} = \mathbf{C}^T$ , which all have zero sum. 

To prove the inclusion  $\supseteq$  implied by Theorem 2.2.6, we first consider the special case that  $G$  is a *tree*.

**Lemma 2.2.8.** *Suppose that  $G$  is a (connected) tree.*

$$\text{Im FRT} \supseteq \ker \sigma \quad (2.4)$$

*Proof.*  $G$  is a tree, so  $m = n - 1$ . Because  $\mathbb{K}^m$  and  $\ker \sigma$  both have dimension  $n - 1$ , we only need to prove that FRT is injective: when FRT has nullity 0, it must have rank  $n - 1$ .

If  $n = 1$ , then the digraph consist of a single node, and no lines. It then follows from (2.1) that the only injection that can be induced is  $\mathbf{p} = (0) \in \mathbb{K}^1$ , so FRT can only be injective.


This proof could benefit from an illustration.

A single-node graph is not connected?

If  $n > 1$ , we will use the fact that the statement holds for any tree with fewer than  $n$  nodes. (*Proof by induction.*)

Suppose that  $f \in \mathbb{K}^m$ , such that  $\mathbf{p} = \text{FRT}(\mathbf{f}) = \mathbf{0}$ . Because  $G$  is a tree, we can<sup>1</sup> pick a leaf  $i \in \mathcal{N}$ , which has a unique line  $\mathcal{L}_k$  connecting  $i$  to some  $j \in \mathcal{N}$ . (We have either  $\mathcal{L}_k = (i, j)$  or  $\mathcal{L}_k = (j, i)$ .)

Only one line is connected to  $i$ , so (2.1) gives:  $p_i = \pm f_k$ . (The sign depends on the orientation of  $\mathcal{L}_k$ .) We assumed  $p_i = 0$ , so we must have  $f_k = 0$ .

By removing node  $i$  and line  $\mathcal{L}_k$ , we obtain a smaller tree, for which the statement already holds. The Flow Response Transformation of this subtree is essentially the restriction of FRT to the set  $\{\mathbf{f} \in \mathbb{K}^m \mid f_k = 0\}$ . Because the restriction is injective, all other coefficients of  $\mathbf{p}$  are also zero. This shows that FRT is injective, and the result follows. 

Make this mapping explicit? The fact that  $p_i = 0$  is required?

*Proof of Theorem 2.2.6.* To prove  $\text{Im FRT} = \ker \sigma$ , it remains to show that

$$\text{Im FRT} \supseteq \ker \sigma \quad (2.5)$$

holds for *any* connected  $G$ , not just for trees.

Since  $G$  is connected, we can choose a minimum spanning subtree: choose  $T \subseteq [m]$  with  $\#T = n - 1$  such that  $G_T = (\mathcal{N}, \{\mathcal{L}_k\}_{k \in T})$  is such a connected subdigraph.


Define  $F_T = \text{Span}\{\mathbf{e}^k\}_{k \in T} \subseteq \mathbb{K}^m$  as the subset of flows on  $G$  that are zero outside of  $G_T$ . Because  $F_T$  is a linear subspace of  $\mathbb{K}^m$ , we have

$$\text{Im FRT} = \text{FRT}(\mathbb{K}^m) \supseteq \text{FRT}(F_T),$$

which reduces the problem to  $\text{FRT}(F_T) \supseteq \ker \sigma$ , which follows from Lemma 2.2.8.

This shows that

$$\text{Im FRT} = \ker \sigma.$$

Because  $\sigma : \mathbb{K}^n \rightarrow \mathbb{K}$  is surjective, it has rank 1. It therefore has nullity  $n - 1$ , or equivalently,  $\ker \sigma \cong \mathbb{K}^{n-1}$ . 

Is this clear enough?

## 2.2.2 Kernel of FRT

Again, assume that  $G$  is connected. In Theorem 2.2.6, we derived an explicit formulation for the image of FRT, showing that  $\text{null FRT} = n - 1$ .

Concerning the kernel of FRT, we already know that  $\mathbf{0} \in \ker \text{FRT}$ , reflecting the fact that zero flow induces zero injection. In the special case that  $G$  is a tree, this is the only such flow. In general, however, the kernel of FRT is much bigger.

introduce loops

**Proposition 2.2.9.** *Suppose that  $G$  is connected. The dimension of  $\ker \text{FRT}$  equals*

$$\text{null FRT} = m - (n - 1).$$

<sup>1</sup>Write  $\text{gr}(i)$  for the number of lines connected to  $i$ .  $G$  is connected, so  $\text{gr}(i) \geq 1$  for each  $i \in \mathcal{N}$ . If no  $i$  exists with  $\text{gr}(i) = 1$ , then  $\text{gr}(i) \geq 2$  for each  $i \in \mathcal{N}$ , giving  $\sum_{i=1}^n \text{gr}(i) \geq 2n$ . On the other hand, each of the  $n - 1$  lines connects exactly two nodes, so  $\sum_{i=1}^n \text{gr}(i) = 2(n - 1) < 2n$ , a contradiction.



*Proof.* This follows directly from the Rank-Nullity theorem, applied to Theorem 2.2.6.

state

**Corollary 2.2.9.1.** *If  $G$  is a tree, then  $\ker \text{FRT} = \{\mathbf{0}\}$ , and  $\text{FRT}$  is a bijection between  $\mathbb{K}^m$  and  $\ker \sigma$ .*

*Proof.* Applying Proposition 2.2.9 with  $m = n - 1$ , we find that  $\text{null FRT} = 0$ , so that  $\ker \text{FRT} = \{\mathbf{0}\}$ . Together with Theorem 2.2.6, we find the result.

talk about loops, use an example graph

Any flow along a *closed loop* results in zero power injection. When interpreting a loop as an element  $\mathbf{f}$  of  $\mathbb{K}^m$ , we must be careful to *flip the sign of  $f_k$  if the line  $\mathcal{L}_k$  is traversed in reverse*.

**Theorem 2.2.10.** *Suppose that  $G$  is connected and that  $(i_1, i_2, \dots, i_p)$  is a closed loop. Then the loop flow  $\mathbf{f} \in \mathbb{K}^m$  defined by:*

$$f_k = \begin{cases} 1 & \text{if } (i_s, i_{s+1}) = \mathcal{L}_k \text{ for any } 1 \leq s < p, \\ -1 & \text{if } (i_{s+1}, i_s) = \mathcal{L}_k \text{ for any } 1 \leq s < p, \\ 0 & \text{otherwise,} \end{cases} \quad (2.6)$$

for each line  $\mathcal{L}_k$ , is an element of the kernel of  $\text{FRT}$ .

this thm only works for Eulerian paths...

*Proof.* We will verify that  $\mathbf{p} = \text{FRT}(\mathbf{f})$  is zero. Choose any  $i \in \mathcal{N}$ .

Because the loop is closed, there is an *even* number (possibly zero) of lines with non-zero flow that connect to  $i$ . This means that the sums in (2.1) cancel each other (note the negative sign for reversed lines in (2.6)), resulting in  $p_i = 0$ .

*Remark.* Because  $\text{FRT}$  is linear, multiplying a loop flow with a scalar  $\gamma \in \mathbb{K}$ , or adding two loop flows, creates a new flow that induces zero injection. (The result of addition is a flow, but in general not a *loop flow*.)

Now that we know the dimension of  $\ker \text{FRT}$ , a natural next step is to look for a *basis* that generates the kernel. Motivated by the previous theorem, we will look for a basis consisting of *loop flows*.

When looking at the previous examples, a logical choice for this basis would be the set of all flows in *loops surrounding the faces contained in the graph*. This approach, which only works for *planar graphs*, will be discussed in the next section.

For now, we would like to find a basis of loop flows for the more general case that  $G$  is connected, but not necessarily planar. We proceed as follows:

**Definition 2.2.11.**

**Theorem 2.2.12.** *The ??? constructed in Definition ??? is a basis for  $\ker \text{FRT}$ .*

*Proof.* Because the number of fundamental loops equals the dimension of  $\ker \text{FRT}$ , one only needs to prove that they are linearly independent. Indeed, for each  $k \in [m] \setminus T$ ,  $\mathbf{f}^k$  is the only fundamental loop for which the  $k$ th element is non-zero. Therefore,  $\mathbf{f}^k$  cannot be written as linear combination of the other fundamental loops.

th: (misschien eerst alleen voor  $K=F_2$ ) the fundamental group

### 2.2.3 Planar Graphs

th: in a planar embedding of a planar graph, the loops surrounding faces form a basis. proof: (in  $F_2$ ): they are linearly independent: these loops are all loops with the property that exactly one face is contained in the loop. ?? proof: (in  $F_2$ ): start with a fundamental basis. choose a loop  $f$  in the fundamental basis. this loop  $f$  contains a number of faces.  $f$  is equal to the sum of the loops around these faces. this shows that  $f$  can be written as linear combination of planar loops. QED

**Corollary 2.2.12.1** (Euler's Formula). *TODO In a planar, connected graph, we have:*

$$v + f - e = 1$$

where  $v$  is the number of vertices,  $e$  is the number of edges, and  $f$  is the number of faces enclosed by edges, excluding the 'exterior face'.

Grid connected iff admittance matrix has full rank?

## *Chapter three*

# Circuit Theory

### 3.1 \*DC Circuits

A short summary of KCL, KVL, Ohm's Law, the Superposition principle, lumped circuits

#### 3.1.1 \*Derivation of KVL& KCL from Maxwell's eq

applying Maxwell's equations to the discrete graph topology

See von  
Meier (2006)  
and Slepian  
(1968)

### 3.2 AC Circuits

Impedance, real & reactive power

## Chapter four

# The Electric Grid

(100W = 16-candela = 200lm = 2.2Watt bij ikea)  
30%? of energy use is transported using the grid  
list of synchronous grids  
complexity  
why interconnect? separate generation and load; economy of scale; security (distributed peak demand); stability;

*This chapter is based on the books Electric Power Systems by von Meier (2006), which provides a clear summary of the working and operation of electric grids, and Electric Power Principles: Sources, Conversion, Distribution and Use by Kirtley (2010), a more quantitative approach to the subject.*

## 4.1 Overview

One could say that the electric grids of this world are some of the largest machines built by humans.

As this system was built by clever engineers, its behaviour is, on a small scale (individual lines, transformers, and so on) *well-understood*. In fact, one of the reasons that all transmission lines, substations and switchboxes look so similar, is to increase the *homogeneity* of the network.

On a larger scale, however, the behaviour of this machine is not always well understood, and .

Because of their scale and complexity

basics, scale, transmission-distribution-?, europe-US, security

## 4.2 Generators

Almost all sources of electric power in the electric grid use an *AC generator* to convert (rotational) kinetic energy to electric energy.<sup>1</sup> At a hydroelectric plant, the weight of water applies direct torque to the water pumps, mechanically connected to the generator shaft.<sup>2</sup> At most other types of plants (including coal-fired and nuclear plants), generators are powered by steam pressure.

The term *AC generator* denotes a specific device that uses *electromagnetic induction* to convert rotational kinetic energy into AC power. Somewhat confusingly, we use the term *generator* to denote *any* energy source connected to the grid, where we consider a power plant (which might house multiple AC generators) as a single generator. Solar parks and lithium batteries are generators, but they do not use an AC generator. They use an AC inverter, which *mimics*, to some extent, the behaviour of a classical AC generator.

coils, 3 phase

## 4.3 Loads

load profiling, load series, fridge duty cycle example, reactive load, power factor

Unlike other utilities like gas and water, the transfer of electrical energy is *instantaneous*.<sup>3</sup> Of course, energy storage does exist,<sup>4</sup> but this energy is not stored as ‘high-voltage AC energy’, but as *potential* (mechanical or chemical) energy. Potential energy needs to be converted before it can be transmitted, which is not instantaneous. When switching on your lights, there will be an *instant* increase in demand, which must be generated somewhere (otherwise it would violate the Law of Conservation of Energy). Of course, via the electric grid, your light bulb is connected to generators, which then start converting an additional 10 W to power the light bulb. But how do the generators know when to increase their output, if you never called them to say that you are turning on your lights?

The answer is called *electric inertia*. A classic AC generator (in a hydroelectric plant, for example) contains a heavy rotor, which is spinning at (a rational fraction of) the grid frequency. Because of its weight, a lot of energy is stored in the spinning of the rotor. When the total load on an AC network is increased, there is no instantaneous

<sup>1</sup>A notable exception is the photovoltaic cell (PV cell) used in solar panels. PV cells produce a direct current, which is converted to AC power at nominal voltage using an *inverter*. Solar inverters are often complicated systems, capable of using battery storage, synchronising with the AC grid and varying PV operating voltage to maximise PV efficiency.

<sup>2</sup>Some hydroelectric plants are *reversible*: their generators can be used as electric motors, pumping water back up into a reservoir. This is a form of large-scale *energy storage*, which can increase the usability of intermittent renewable energy sources.

<sup>3</sup>Within the limits of special relativity, of course. That is, while the drift speed electrons is nowhere near the speed of light, the actual *signal* propagates at about two thirds the speed of light, depending on the type of cable.

<sup>4</sup>Most commonly as *reversible* hydro-electric generators; other examples include hydrogen storage (electrolysis of water produces hydrogen and oxygen, which can be stored and combusted at a later time) and lithium storage (very large phone batteries) (some electric vehicles can also return energy back to grid!)

increase in burning of fuel, flowing of water, or otherwise. Instead, this increase in power demand will 'take' its energy from the *inertial energy* of all rotational AC generators in the grid, *slowing down* their rotation. As a result, the AC frequency of the entire grid starts slowing down. When grid operators notice a drop in AC frequency (we are talking about differences on the order of 0.001 Hz here), they can increase the amount of fuel being burned, open water valves or lift control rods from between radioactive cores to increase the amount of energy converted by the AC generator. This will start to increase the AC frequency again, until it settles at the predetermined utility frequency (60 Hz in North America and Northern South America; 50 Hz in the rest of the world, with some exceptions). Most modern AC generators have an automatic feedback loop to control the steam valve, to allow for frequency adjustments on the smallest scale.

## 4.4 Transmission

Should cover: lines, transformers, circuit breakers, grid security

### 4.4.1 DC transmission

### 4.4.2 3-phase transmission

The AC grid has 3 phases, but it is very common to model the grid as a single-line network (with a global, zero-impedance ground). Von Meier mentions material that justifies this change.

If you live in mainland Europe, North America, , your wall socket will have *two* connectors. Most modern sockets also have a third connector, the *ground wire*.

This makes sense, since most electrical devices only need a *potential difference* (between *two* wires) to function. In the early days of transmission systems, however, this caused a problem for factories using AC motors to power their production line. When a (single-phase) AC current is used to power a motor, the amount of *torque* <sup>5</sup> is not constant: when the potential difference is zero, which happens twice every 1/50<sup>th</sup> of a second, no electric field is present in the armature windings, and no torque is applied to the rotor.

To solve this problem, both the AC generator and AC motor are equipped with *three* identical sets of armature windings, each oriented 120° relative to the others. One end of each winding is connected to the common ground, and the remaining three connection points form the *three-phase connection* between generator and motor.

As the generator rotor is moving, there will always be one armature winding which is close <sup>6</sup> to being perpendicular to the rotor windings, and will therefore have a relatively high induced current.

<sup>5</sup>i.e. rotational force. In most systems, torque is proportional to *change in rotational velocity* (change in rpm).

<sup>6</sup>within 30°

en waarom is dat een probleem?

In fact, when writing down the three currents in exact form (three sinusoids with the same frequency and magnitude, with phases  $0^\circ$ ,  $120^\circ$  and  $240^\circ$ ), we find that *the sum of their squares*, i.e. the total amount of transmitted power, *is constant!* Although the amount of power transmitted on just one of the phases (square of the sinusoid current) is not constant, the combination of the three is.

This means that the torque of a motor, which is the sum of torques applied by each armature winding, is constant.

Nu weten we ook wat het verschil is tussen ground en de linkerdraad!

When looking at AC transmission systems, you will always find three identical copies of the same component. For example, high-voltage AC transmission lines always have three, six or nine wires, which are identical in material, thickness and length.

There are a number of reasons to build transmission systems this way. One benefit of having three copies of the exact same network is that they will behave the same way, saving grid operators up to two thirds of potential headaches!

What we just described is a *Wye* connection

om ons heen

### Single-line approximation

Move to next 5?

#### 4.4.3 Line failures

When a transmission line stops transmitting power, we speak of a *line failure*. In most cases, a line failure is not caused by a broken or molten wire, but by a disconnection at one of its ends, as a safety measure. Some line failures are caused by a fault: a sudden abnormal peak in current, caused by anomalies like fallen trees or lightning strikes. A high current is detected by a *circuit breakers*, which then automatically breaks its connection. A household fuse is an example of a circuit breaker, although modern circuit breakers use a mechanical switch (which be reset, instead of requiring a replacement fuse). In high-voltage systems, circuit breakers can be quite advanced, sometimes using pressurised gas or oil to prevent arcing inside the switch.

Another type of line failure, the one most relevant to this report, is an *overload*. All transmission lines have a *thermal limit*: a maximum current that the line can sustain without risking overheating, causing sagging or even melting of transmission cables. To prevent these dangerous scenarios, transmission lines automatically disconnect when the current exceeds the predetermined *line capacity*.

or stability limit

It is important to note that grid operators cannot control the amount of current - and therefore - power that flows through a transmission line, grid operators can only connect or disconnect the line from the grid. The impedance of a wire does not act as a *bottleneck* (like a small-diameter pipe would do in an irrigation network). From Ohm's law ( $ZI = V$ ), one could mistakenly conclude that the amount of current passing through a transmission line is inversely proportional to its resistance. However, the electric potential ( $V$ ) in this equation is *not* the potential between the wire and the ground (e.g. 220 kV), but rather the potential difference between the two ends of the

wire (which is not zero!). This difference (known as *line drop*) is quite low, compared to the potential between one of the ends and the ground (220 kV transmission lines usually have a 1% line drop). The amount of current carried by a wire is dominated by the current being 'generated' and 'used' at its ends.

check

not the case for DC transmission?

dynamic rating: modern transmission lines will allow a current beyond its threshold for a short while, and will have different ratings for different weather conditions

## 4.5 Power Flow Analysis

historic note, slack bus, distributive slack, DC approximation, optimal power flow

## 4.6 Transmission grid operation

The transmission network is a crucial

The transmis

In societies that

Historically, failures of transmission network have had dramatic effects. The effects of such outages are even visible from space, since almost every light source indirectly depends on a functioning transmission network.

Luckily, TODO where a power-outage would be life-threatening, or has significant economic impact, often have backup generators in place.

In modern hospitals, medical equipment often has a built-in battery to sustain relatively short power cuts. (When unplugged by accident, for example.) Hospitals also use two sets of power lines with independent protection: one for essential equipment, and one for computers, lights, phone chargers, et cetera.

It should come as no surprise that the transmission network requires constant monitoring to ensure that it is working properly.

When the first power grids were built, grid security was ensured by *redundancy*. Transmission lines were designed to carry currents much greater than predicted. One of the criteria for building a network was *N-1 contingency*: the network should remain operational after the failure of *any* line. In graph theory, this is equivalent to building a 2-edge-connected graph.

historic note

### 4.6.1 Power islanding

Because nodes often house both loads and generators, the disconnection of a single node, or of a subset of nodes, does not always lead to a power outage, since local power generation might be sufficient to serve the load. This situation, where a subsection of the transmission network still operates after being disconnected, is called a *power island*.

Since the power island and the remaining network have been operating independently



of each other, it is likely that their AC phase angles no longer line up.<sup>7</sup> Unless this phase drift is corrected for (by temporarily increasing or decreasing the AC frequency on either side), the power island cannot be reconnected, since this phase drift likely exceeds the power angle limit of a new transmission line.

adsf

---

<sup>7</sup>This misalignment likely occurs right after the disconnection, when the total generation in the power island is substantially higher or lower than the total load. Until this mismatch has settled, the AC frequency will be higher or lower, respectively, than the target frequency (say, 50 Hz).

## 4.6.2 The energy market

intro. Very simplified world:

Every hour, all parties involved in the generation and transmission of power come together, to decide *what the configuration during the following hour will be*. For the sake of simplicity, we will assume that each power plant (renewable or non-renewable) is owned by its own company, and that the entire transmission network is owned by a single grid operator.

### Phase one: offering prices

First, all generators offer to supply energy during the coming hour *for a certain price per kWh*. Generally, company A, which owns a wind farm, will offer their energy for a lower price than company B, which owns a coal plant. The price offered by company A is lower because a wind farm has zero *marginal cost* - the cost of generating an additional unit of electricity, once the turbine has been built. No fuel or labour is needed to generate power using a wind turbine, it simply needs to not be turned off.

Besides marginal cost, there are two more factors that influence the offered price:

- Company A needs to pay back their initial investment, which increases the offered price.
- Government subsidies, which promote the use of low-carbon energy, reduce the offered price.

In general, one can assume that the price offered for renewable energy is close to zero. In some cases, the subsidies are greater than all other costs, and energy is offered for a *negative price*. This has the counter-intuitive effect that a grid operator actually *earns money* by buying electricity from that company.

Energy from company B is generally more expensive, since it has a marginal cost (price of coal, labour wages, and so on), on top of paying back the investment.<sup>8</sup>

Misschien is dit een goede plek om de *environmental cost* van elk type generator te geven

Besides offering their marginal price, generators will also state their *generation capacity*.<sup>9</sup> For some generators, this will always be the same amount. For a solar park, however, this capacity varies drastically, and needs to be estimated.

### Phase two: grid operator

Now that all generators have offered a price, the grid operator needs to decide where to buy its energy from. Grid operators have a fairly good estimate for the load (energy

<sup>8</sup>In some cases, coal plants offer their electricity for a lower, or even negative, price, to avoid power off the plant. With the exception of open-cycle gas turbines, turning on non-renewable energy plants is expensive, and might take several hours. It might be cheaper for company B to offer their energy for free for one hour than to turn off the plant.

<sup>9</sup>This use of the word *capacity* is entirely different from the *capacity* of a capacitor, used in electrical engineering.

15 March 2019, 11:00–12:00		
<i>generator</i>	<i>offered price</i>	<i>requested output</i>
Sally's Solar Park	4 €/MWh	115 MW / 115 MW
Chris's Coal Plant	122 €/MWh	0 MW / 240 MW
Nellie's Nuclear Plant	45 €/MWh	1387 MW / 2500 MW
Steven's Solar Park	-2 €/MWh	23 MW / 23 MW
⋮	⋮	⋮

**Table 4.1:** A small section of a fictional configuration.

demand) during the coming hour, based on the current load, historical load series, weather forecasts, sporting events, television programme schedules, and so on. Such a model is called a *load profile*.

By design, the total generation capacity is much greater than the expected load, so running every generator at full capacity would be problematic. As a grid operator, we need to tell each generator at what percentage of their capacity they should operate.

A complete set of generator instructions, called a *configuration*, might look something like Table 4.1. Note that generators could be told to operate at 0% of their capacity, which is equivalent to powering off the generator completely.

Some configurations are more expensive than others, and some will result in more greenhouse gas emissions than others. Perhaps surprisingly, most configurations are not even *admissible*: using them would cause some transmission lines to be overloaded, which could even result in a blackout.

More precisely, a configuration is called *ready to deploy* if it satisfies the following three conditions:

*possible*: For each generator, the power output dictated by a configuration must be a non-negative number, no greater than the maximum capacity of the generator.

*balanced*: When the dictated configuration is applied, total generation must equal total load, together with line losses.<sup>10</sup>

*admissible*: When the dictated configuration is applied, no line should be overloaded.

To determine whether a configuration is *admissible*, the grid operator can simply *calculate the line flows* that would be induced by that configuration, using a Power Flow (PF) algorithm, and check for any overloaded lines. Because power flow physics are quite well-understood, these results are accurate.

<sup>10</sup>Of course, the total load is not perfectly constant for one hour. To accommodate for this, the grid operator designates a single *load following* generator, which will vary its output continually to make sure that the total demand is met exactly. (This is equivalent to maintaining a constant AC frequency!) The bus that this generator is connected to is called the *slack bus* of the transmission network.

load profile  
plotje

why? winter  
and incident  
load

stats: het  
percentage  
van totale  
capaciteit  
dat wordt  
gebruikt ligt  
tussen ?%  
en ?%.

admissible  
is niet ja of  
nee

accuracy

geschiedenis  
van PF:  
modellen

## OPF

We can easily find a configuration that is both possible and balanced. First, set all generators to maximum capacity. We now have a *possible* configuration. By design, the total generation of this configuration is much greater than the total load. By scaling the output of all generators with the same factor  $0 \leq \lambda \leq 1$ , the configuration remains *possible*, and by the intermediate value theorem, a  $\lambda$  exists such that the configuration is *balanced*.

When trying out different *possible, balanced* configurations randomly, we will find that almost all of them are inadmissible; the subset of admissible configurations is actually quite small, and finding *any* ready-to-deploy configuration is a lot of work.

Once a ready-to-deploy configuration has been found, the grid operator now wants to minimise economic and environmental cost. Given this initial configuration, the associated cost can be calculated, since all generators have offered their price, and their environmental impacts are known. This ready-to-deploy configuration is not unique, and by varying the configuration only slightly, the configuration remains ready to deploy.<sup>11</sup> By doing so, we might be able to reduce the (environmental) cost! By repeating this process, a local minimum can be found.

The problem of

*finding a ready-to-deploy configuration  
that minimises the associated cost*

is called the *Optimum Power Flow (OPF)* problem.

Even with modern-day computers, solving this problem is a difficult task indeed, and is often simplified by making a slight modification to our process. Instead of using the Power Flow (PF) algorithm to check a configuration's admissibility, we use the so-called *Linearised Power Flow (LPF)* algorithm to check linear admissibility. This linearised version can be computed much more quickly, with only a small loss in accuracy. We will derive the equations describing these two algorithms in Chapter 5, and compare their results.

linear bal-  
ance

With our slight modification, we restate our problem as:

minimise    *associated cost*  
subject to   *possibility*  
and            *balance*  
and            *linear admissibility*

which is known as the *Linear Optimum Power Flow (LOPF)* problem. As suggested by the notation, this optimisation problem falls in the more general class of problems solvable using *linear programming*. First studied by Fourier in 1827, the field has seen many developments, most notably the *simplex* solution method developed by G. Dantzig in 1947.<sup>12</sup> Nowadays, several high-performance linear programming solvers have

<sup>11</sup>As we will later learn, the function that maps a configuration to the vector of line flows that it induces is *continuous*. The set of vectors where each line flow is  $< 100\%$  is an *open* box, and so its inverse image (the set of configurations that are ready to deploy) is also open.

<sup>12</sup>For the *simplex method*, see Matoušek and Gärtner (2007) .

been created, including the open source GNU Linear Programming Kit, which was used in this project.

Je kan de eisen van OPF naar beneden schalen om lineaire admissibility te krijgen (bv de contingency factor!)

## Chapter five

# Modelling Transmission Networks

In this Chapter we will derive the *Linear Power Flow* transformation: a linear map from the vector of power injections at the buses to the vector of currents flowing through the lines of the network. This equation can be derived explicitly by constructing an electric circuit that represents the whole transmission network and everything connected to it, and applying Ohm's Law and Kirchoff's Laws to relate line currents to power injections. We linearise the resulting *node flow equations* to find the LPF matrix (page 44).

Using this linear map, we can transform the normal distribution of stochastic injections to a Gaussian distribution of line flows. Using the results of Chapter ??, we can estimate the overload probability of each line, resulting in a ranking of most vulnerable lines. Additionally, for each such line, we compute the most probable injection to cause the failure, and simulate the subsequent *cascading failures*.

intro state & structure

The grid structure remains unchanged during normal operation, while the grid state is continually changing over time. For example, an important aspect of grid operation is *load profiling*: examining and predicting the total load connected to a node, as a function of time. As a result of changing loads, the flow of power in a grid is constantly changing.

One example of a change in grid structure is a *line failure*, which can be modelled as the removal of an edge from the graph. In some cases, the removal of an edge from the graph result in an unconnected graph (i.e. there exist two nodes with no sequence of lines connecting them). This scenario is called *power islanding*. Most transmission networks are designed in such a way that no single (or double) line failure can cause power islanding or a blackout, by increasing the *edge-connectivity* of the graph.

In the case of a *line overload*, however, a line failure is caused by an exceptionally high power flow, as a result of high supply or demand.<sup>1</sup> The failure of an overloaded line will cause a redistribution of power flow, since the power flowing through the failed line now needs to 'find another path' between the nodes. In a highly stressed network, this redistribution can cause a second failure, which can then cause a third failure, and so

<sup>1</sup>These high power injections are not necessarily located at the two endpoints of an overloaded line; it could also be a grid-wide pattern of power injections, all adding up to a high power flow on that line. We will study the *most likely power injection* in Chapter ??.

on, eventually causing a blackout. We will study these *cascading failures* in Chapter ??.

## 5.1 Grid structure

A transmission grid is modelled as a directed graph  $(\mathcal{N}, \mathcal{L})$ . As vertices we take the *nodes* of the network, which are those points where transmission lines connect to a generator, load, or to each other. Nodes are electrically distinct, in the sense that there is some non-zero impedance between them, allowing them to sustain a potential difference. In a network of  $n$  nodes, they are represented by the natural numbers  $1, \dots, n$ , in arbitrary order.

A pair of two nodes  $(i, j)$  is contained in the set of edges  $\mathcal{L}$  iff there is a transmission line connecting the nodes, and  $i < j$ . (Note that by construction, this transmission line has non-zero impedance.) The choice of line orientation can be arbitrary, but we fix the orientation to  $i < j$ . In a network of  $m$  lines, lines are labeled  $\mathcal{L}_1, \dots, \mathcal{L}_m$ , in arbitrary order.

Vertices will be called nodes, and edges will be called lines.

Given a directed graph with  $n$  nodes and  $m$  lines, we define the edge-vertex incidence matrix  $\mathbf{C} \in \mathbb{R}^{m \times n}$  as:

$$C_{k,i} = \begin{cases} 1 & \text{if } \mathcal{L}_k = (i, j) \text{ for some } j \in [n], \\ -1 & \text{if } \mathcal{L}_k = (j, i) \text{ for some } j \in [n], \\ 0 & \text{otherwise.} \end{cases}$$

The ordered set of lines is uniquely defined by the edge-vertex incidence matrix.

transformer normalisation

We model transmission lines as time-invariant impedances, which are assumed to be constant under any electric potential and current, allowing us to apply Ohm's Law. Instead of the impedance  $Z$  of a line, we use its *admittance*  $Y = 1/Z \in \mathbb{C}$ ,<sup>2</sup> and Ohm's Law becomes:

$$\mathbf{I} = \mathbf{V}\mathbf{Y}$$

This allows us to define the admittance between two unconnected nodes as 0. (i.e. no current is induced by a potential difference.) We now construct the *admittance matrix*  $\mathbf{Y} \in \mathbb{C}^{n \times n}$ , where  $Y_{i,j}$  is the admittance between nodes  $i$  and  $j$ . Note that  $\mathbf{Y}$  is a symmetric matrix, with only  $2m$  non-zero entries.

We also define  $\boldsymbol{\eta} \in \mathbb{C}^m$  as the *admittance vector*, where  $\eta_l$  is the admittance of  $\mathcal{L}_l$ , for each  $l \in [m]$ . Equivalently, one can write  $\boldsymbol{\eta} := \mathbf{Y}_{\mathcal{L}}$  for each  $l \in [m]$  since each  $\mathcal{L}_l$  is a tuple of node indices.

**Definition 5.1.1.** To summarise, an  $(n, m)$ -grid structure is defined as a tuple  $((\mathcal{N}, \mathcal{L}), \mathbf{C}, \boldsymbol{\eta})$  where:

<sup>2</sup>Written in Cartesian form,  $Y = G + iB$ , where  $G$  is the conductance, and  $B$  the susceptance of a line. Both have unit siemens (S), or mho (the reverse of 'ohm'), defined as  $1 \text{ S} = 1 \Omega^{-1}$ .

We model the line protection mechanism as deterministic: overload causes instantaneous failure.

Require the graph to be connected? How about power islands?

Not necessary

$\mathbf{Y}$  is not used very often and conflicts with the Nodal admittance matrix (wiki)

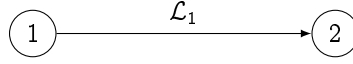


**Figure 5.1:** The simple *two-node* transmission network of two nodes and one line.

- $n = \#\mathcal{N}$  is the number of nodes;
- $m = \#\mathcal{L}$  is the number of lines;
- $(\mathcal{N}, \mathcal{L})$  is a connected directed graph with  $\mathcal{N} = [n]$ ;
- $\mathbf{C} \in \mathbb{R}^{m \times n}$  is the edge-vertex incidence matrix of  $(\mathcal{N}, \mathcal{L})$ ;
- $\boldsymbol{\eta} \in \mathbb{C}^m$  is the line admittance vector.

table

**Example 5.1.2** (Two-node network). A very simple transmission network is one with just two nodes, and a single line connecting them. This *two-node network* is drawn in Figure 5.1. Although real networks are much bigger, this example is useful to illustrate some of the concepts introduced in this chapter.

We have:

$$\begin{aligned}\mathcal{N} &= \{1, 2\} \text{ and} \\ \mathcal{L} &= \{\mathcal{L}_1\} \text{ with } \mathcal{L}_1 = (1, 2).\end{aligned}$$

Since  $n = 2$  and  $m = 1$ ,  $\mathbf{C}$  is a  $1 \times 2$  matrix:

$$\mathbf{C} = \begin{pmatrix} 1 & -1 \end{pmatrix}.$$

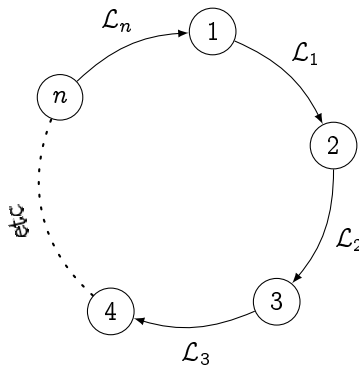


**Figure 5.2:** The *n-loop* transmission network with  $n$  nodes and  $n$  lines.

**Example 5.1.3** (Loop network). A less trivial transmission network is the *n-loop network*, shown in Figure 5.2. It consists of  $n$  nodes, connected in a circular fashion (using  $n$  lines).



Note that this network is 2-edge connected, meaning that the network remains connected when any edge is removed. (Although removing *any* two lines will disconnect the network.)

We have:

$$\mathcal{N} = \{1, \dots, n\} = [n] \text{ and}$$

$$\mathcal{L} = \{\mathcal{L}_1, \dots, \mathcal{L}_n\} \text{ with } \mathcal{L}_i = (i, i+1) \text{ for } 1 \leq i < n \text{ and } \mathcal{L}_n = (n, 1).$$

Since  $m = n$ ,  $\mathbf{C}$  is an  $n \times n$  matrix:

$$\mathbf{C} = \begin{pmatrix} 1 & -1 & & & & \\ & 1 & -1 & & & \\ & & 1 & -1 & & \\ & & & \ddots & \ddots & \\ & & & & 1 & -1 \\ -1 & & & & & 1 \end{pmatrix}.$$

(All unspecified elements are 0).

Note that rows of  $\mathbf{C}$  correspond to lines of the network. T

**Example 5.1.4** (SciGRID Germany). TODO

Mostly for fun, and to emphasise that the dataset can be modelled in this form.  
The dataset will be treated in detail in Part II.  
Will also emphasise that in most real networks,  $m > n$ .

T

## 5.2 Power grid state

TODO, I is directed along the graph edges

**Definition 5.2.1.** To summarise, a *grid state* of an  $(n, m)$ -grid structure is defined as a tuple  $(\mathbf{S}, \mathbf{V}, \mathbf{I})$ , where

- $\mathbf{S} \in \mathbb{C}^n$  is the *complex power injection vector*;
- $\mathbf{V} \in \mathbb{C}^n$  is the *bus voltage vector*;
- $\mathbf{I} \in \mathbb{C}^m$  is the *line current vector*.

I could be left out of the grid state, since it is uniquely determined by  $\mathbf{V}$  and the structure.

U instead of V? Not common in lit

## 5.3 State validity

Given an  $(n, m)$ -grid structure  $((\mathcal{N}, \mathcal{L}), \mathbf{C}, \boldsymbol{\eta})$ , only some states are physically possible. A state that satisfies Kirchoff's Laws and Ohm's Law is called *valid*. Since we are studying a real-world system, we are mainly interested in states that are valid, or at least close to being valid (in the sense of *DC-valid*, see Section 5.5).

### 5.3.1 Electrical representation

An  $(n, m)$ -grid structure  $((\mathcal{N}, \mathcal{L}), \mathbf{C}, \boldsymbol{\eta})$  represents an electrical circuit, consisting of impedances and AC sources. A *valid* grid state  $(\mathbf{S}, \mathbf{V}, \mathbf{I})$  corresponds to a physical state of the circuit. Given the mathematical structure, we will construct the electric circuit in two layers, as follows:

In the first layer, each node  $i$  in  $\mathcal{N}$  becomes a node in the circuit. The value of  $V_i$  is the electric potential of that node, relative to ground.

A line  $\mathcal{L}_k = (i, j)$  is modelled as an impedance<sup>3</sup> ( $\text{---}\square\text{---}$ ) with admittance  $\eta_k$  between the two nodes  $i$  and  $j$ . The value of  $I_k$  is the current flowing through the impedance from  $j$  to  $i$ .

check sign

See Figure 5.3 for the first constructed layer. This is not yet the final circuit: we have not yet added generators and loads to the circuit. Also, the transmission lines have no return wire. This means there is no closed loop between two nodes, and therefore no energy can be transmitted.

To construct the second layer, we add a new component to each node  $i \in \mathcal{N}$ , which can be seen as the collection of AC sources (generators) and impedances (loads), connected in parallel between the node and ground. Since an exact configuration<sup>4</sup> of loads and generators connected to the node is not important, we will simply state that this component:

- sustains a potential difference (which is  $V_i$ );<sup>5</sup>
- either supplies or draws a current, such that the amount of power generated or consumed by the component equals  $S_i$  (when  $S_i$  is positive or negative, respectively).

We will call this aggregation of generators and loads a *power injector* ( $\text{---}\textcircled{\curvearrowright}\text{---}$ ).

Each power injector is connected to a node on one end, and to a ground terminal on the other. In electric circuit theory, a ground terminal represents a direct connection to a universal ground: the zero reference of electric potential. One could say that between two different ground terminals, there exists a zero-resistance link connecting the two. We now have a simple closed circuit between any two nodes connected by a transmission line, consisting of a power injector for the first node, an impedance between the two nodes, a power injector for the second node and a ground link back to the first node.

The complete, two-layer model is shown in Figure 5.4.

<sup>3</sup>complex-valued resistor

<sup>4</sup>This would be a circuit comprising the medium and low-voltage networks connected to the node, including every generator, fridge and phone charger that it serves. This is a common (and necessary) abstraction in power grid analysis.

<sup>5</sup>In physical systems, the *operating voltage*  $|V_i|$  (remember that  $\mathbf{V}$  is complex) can be controlled by power plant operators by adjusting excitation current of a generator. The *phase angle*  $\theta_j = \text{Arg}(V_j)$  can be controlled by adjusting the amount of energy (steam) supplied to a generator.

Both methods are an indirect form of control and the effects are very complex in nature, since the operating voltage and phase angle of one node is inherently linked to that of all other nodes in the network. In fact, *maintaining* a constant operating voltage and phase angle is a complicated task, requiring continuous adjustments to generator operation. See Section 4.3 of von Meier (2006) for a more detailed description.

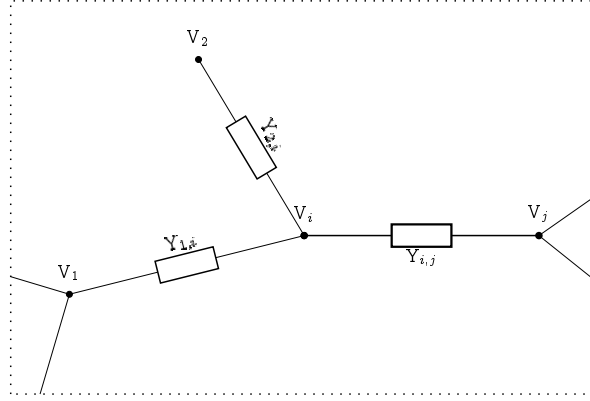


**Figure 5.3:** A section of a transmission network, showing the line  $(i, j)$ . Two more nodes, both connected to  $i$ , are also shown. Note that this is only one layer of the electric circuit used in the model. In the full model (Figure 5.4), each transmission line forms a closed circuit, allowing current to flow.

Justify conductive ground wire in a 3-phase system

### 5.3.2 Kirchoff's Voltage Law (KVL) & Ohm's Law

For each line  $\mathcal{L}_k = (i, j)$ , we can apply Kirchoff's Voltage Law to the loop “ground  $\rightarrow i \rightarrow j \rightarrow$  ground”, as shown in Figure 5.4. This gives us:

$$V_i + \Delta V_k + -V_j = 0,$$

where  $\Delta V_k$  is the electric potential of the line impedance. This potential relates to the line current according to Ohm's Law:

$$I_k = \Delta V_k \cdot \eta_k = (V_j - V_i) \cdot \eta_k.$$

Since the  $k$ th row of  $\mathbf{C}$  (which corresponds to the line  $\mathcal{L}_k = (i, j)$ ) has two non-zero entries:  $C_{k,i} = 1$  and  $C_{k,j} = -1$ , we can write:

$$I_k = (V_j - V_i) \cdot \eta_k = -(\mathbf{C}\mathbf{V})_k \eta_k.$$

This holds for every  $k \in [m]$ , and this system of equations can be written compactly as:

$$\mathbf{I} = i \operatorname{diag}(i\eta) \mathbf{C}\mathbf{V}$$

Written in this form, we see that when  $i\eta$ ,  $\mathbf{C}$  and  $\mathbf{V}$  are purely real, then  $\mathbf{I}$  is purely imaginary. Physically, this means that line current is always  $90^\circ$  out of phase with node voltage. (Or it means that current is out of phase with voltage differences? Which are voltage angle differences?)

Writing node voltages in a circuit already implies that KVL holds.

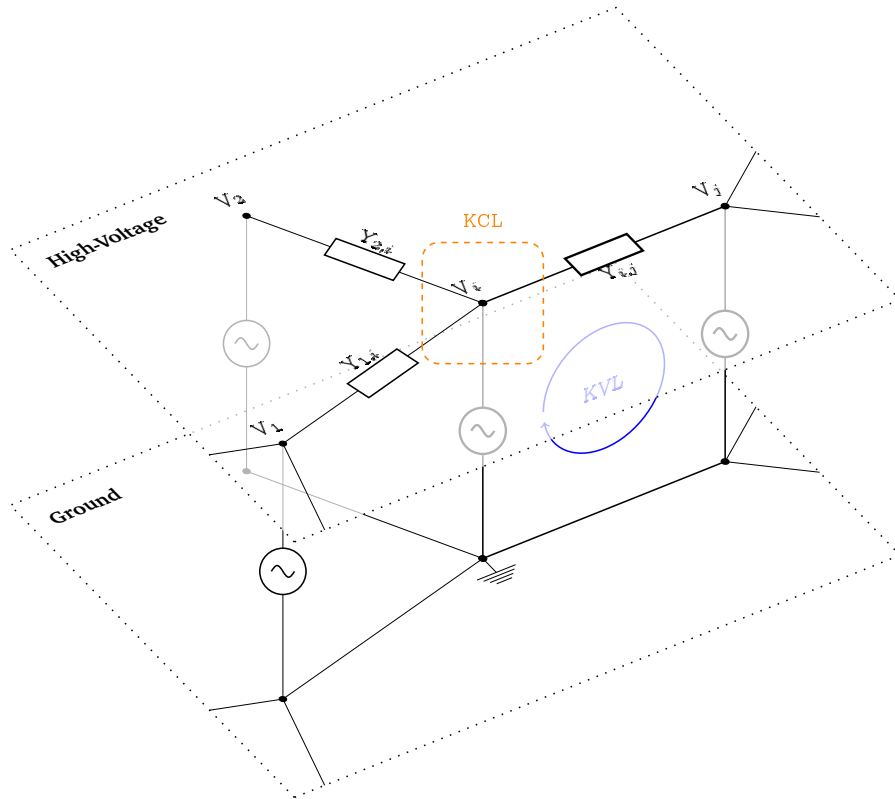


**Figure 5.4:** The electric model of the transmission network, showing the line  $(i, j)$  and two other nodes. A node is represented by a single component  $(-\textcircled{?}-)$ , which is the aggregation of all generators and loads connected to that node. A transmission line is modelled as an impedance  $(-\square-)$ , a complex-valued resistor. The ground 'wires' have zero resistance.

**KVL** is applied to each **line**, by traversing the loop drawn in blue.

**KCL** is applied to each **node**, by summing all currents entering and leaving the orange area.

### 5.3.3 Kirchoff's Current Law (KCL)

Using KVL and Ohm's Law, we found a relation between line current and node voltages. We can use KCL to

Let's apply KCL to every high-voltage node in the electric circuit, as shown in Figure 5.4. This gives us:

$$\mathbf{S} + (\mathbf{C}^T \mathbf{I})^* * \mathbf{V} = \mathbf{0}$$

which is the sum of line currents entering the node, minus the sum of line currents leaving the node.

Show derivation of (S-KCL) from KCL in the last illustration

### 5.3.4 Validity conditions

intro

**Definition 5.3.1.** Given an  $(n, m)$ -grid structure  $((\mathcal{N}, \mathcal{L}), \mathbf{C}, \boldsymbol{\eta})$ , a grid state  $(\mathbf{S}, \mathbf{V}, \mathbf{I})$  is *valid* if it satisfies the *KVL-Ohm equality*:

$$\mathbf{I} = i \operatorname{diag}(i\boldsymbol{\eta}) \mathbf{C} \mathbf{V} \quad (\text{KVL-Ohm})$$

and the *KCL equality*:

$$\mathbf{S} + (\mathbf{C}^T \mathbf{I})^* * \mathbf{V} = \mathbf{0}. \quad (\text{S-KCL})$$

*Remark.* In physical terms, the *KVL-Ohm equality* states:

Each line  $\mathcal{L}_k = (i, j)$  satisfies Ohm's Law ( $\mathbf{l} = \mathbf{V}\mathbf{Y}$ ), where:

$$\mathbf{l} = \mathbf{I}_k, \quad \mathbf{V} = \mathbf{V}_i - \mathbf{V}_j, \quad \mathbf{Y} = \boldsymbol{\eta}_k$$

and the *KCL equality* states:

At each node  $i$ , the sum of power injected at the node,  $\mathbf{S}_i$ ,  
and power injected from the grid, must equal 0.

**Proposition 5.3.2.** Given a grid structure and state as in Definition 5.3.1, the following are equivalent:

- i. The grid state is valid.
- ii. The grid state satisfies (KVL-Ohm) and (S-KCL).
- iii. The grid state satisfies (KVL-Ohm), and each node  $i$  satisfies the node flow equation:

$$\mathbf{S}_i = i \sum_{j=1}^n \mathbf{L}_{i,j}^* |\mathbf{V}_i| |\mathbf{V}_j| e^{i(\theta_i - \theta_j)} \quad \text{for each } i \in [n], \quad (5.1)$$

$$\text{where } \mathbf{L} = \mathbf{C}^T \operatorname{diag}(i\boldsymbol{\eta}) \mathbf{C} \quad (5.2)$$

and  $\boldsymbol{\theta} \in \mathbb{R}^n$  is the vector of voltage angles, i.e.  $\theta_j = \text{Arg}(V_j)$  (the principle argument of  $V_j$ ). We call  $\mathbf{L}$  the nodal susceptance matrix (Ronellenfitsch et al., 2017).

*Remark.* Note that (5.1) does not depend on  $\mathbf{I}$ . This means that a valid state is uniquely determined by  $\mathbf{S}$  and  $\mathbf{V}$ , since  $\mathbf{I}$  can be computed from  $\mathbf{V}$  using (KVL-Ohm).

*Remark.* Writing in real and imaginary components, we get the node flow equations for real and reactive power for each node  $i \in [n]$ :

$$P = \Re(S_i) = \sum_{j=1}^n |V_i||V_j| \left[ \Re(M_{i,j}) \cos(\theta_i - \theta_j) + \Im(M_{i,j}) \sin(\theta_i - \theta_j) \right] \quad (5.3)$$

$$Q = \Im(S_i) = \sum_{j=1}^n |V_i||V_j| \left[ \Re(M_{i,j}) \sin(\theta_i - \theta_j) - \Im(M_{i,j}) \cos(\theta_i - \theta_j) \right] \quad (5.4)$$

In literature on the subject, the node flow equation is often given in this form.

$\mathbf{M}$  should be  $\pm i\mathbf{L}$

We will later study so called *DC-valid* grid structures, where the values of  $\mathbf{M}$  are purely imaginary. If so, (5.3) simplifies to:

$$P = \Re(S_i) = \sum_{j=1}^n \Im(M_{i,j}) |V_i||V_j| \sin(\theta_i - \theta_j),$$

which tells us that in a network of just two nodes and one line with purely imaginary admittance, the amount of real power transmitted is proportional to  $\sin(\theta_2 - \theta_1)$ .<sup>6</sup>

*Proof.* (i)  $\iff$  (ii) is true by definition.

Suppose the grid state satisfies (KVL-Ohm). We have

$$\begin{aligned} \mathbf{S} + (\mathbf{C}^T \mathbf{I})^* * \mathbf{V} &= \\ \mathbf{S} + (i\mathbf{C}^T \text{diag}(i\boldsymbol{\eta})\mathbf{C}\mathbf{V})^* * \mathbf{V} &= \\ \mathbf{S} + (i\mathbf{L}\mathbf{V})^* * \mathbf{V} &= \mathbf{0} \end{aligned}$$

iff for each  $i \in [n]$

<sup>6</sup>The quantity  $\theta_2 - \theta_1$  is called the *power angle* of the transmission line, a common measure of the amount of power being transmitted. As discussed in Section ??, a power angle greater than  $45^\circ$  will cause the nodes to lose synchronicity, making power transmission between the two nodes impossible. For long lines (over 100km), this *stability limit* places an upper limit on the amount of power that a line can transmit. For shorter lines, the *thermal limit* dominates.

is this Newton's heat equation with  $\mathbf{M}$  the discrete Laplacian?

$$\begin{aligned}
S_i &= - \left( \sum_{j=1}^n iL_{i,j} V_j \right)^* V_i \\
&= - \left( \sum_{j=1}^n -iL_{i,j}^* V_j^* \right) V_i \\
&= i \sum_{j=1}^n L_{i,j}^* V_i V_j^* \\
&= i \sum_{j=1}^n L_{i,j}^* |V_i| e^{i\theta_i} |V_j| e^{-i\theta_j} \\
&= i \sum_{j=1}^n L_{i,j}^* |V_i| |V_j| e^{i(\theta_i - \theta_j)},
\end{aligned}$$

proving (ii)  $\iff$  (iii). ✍

## 5.4 Power Flow

In the previous section, we derived a fundamental result: the *node flow equation* (5.1). Recall from Section ?? that the *power flow problem* entails the following:

*Given an  $(n, m)$ -grid structure  $((\mathcal{N}, \mathcal{L}), \mathbf{C}, \boldsymbol{\eta})$ , and a power injection  $\mathbf{S}$ ,  
find  $\mathbf{V}$  and  $\mathbf{I}$  such that  $(\mathbf{S}, \mathbf{V}, \mathbf{I})$  is a valid state.*

Or put more simply:

*Given the production or consumption at each node,  
find the current flowing through each line.*

It turns out that the easiest way to solve this problem is to solve the node flow equation to obtain  $\mathbf{V}$ . Once  $\mathbf{V}$  is known, one can easily compute  $\mathbf{I}$  using KVL-Ohm, giving a state  $(\mathbf{S}, \mathbf{V}, \mathbf{I})$  that is valid by construction.

The node flow equation is a system of non-linear equations, and no closed-form solution is known to exist in general. Fortunately, solving the node flow equation is essentially a root-finding problem. This means that well-established techniques, such as the Newton-Raphson algorithm, can be used to find a numerical solution.

Difficulty of finding initial values that convergence: flat start. Is DC approx used as initial value?

## 5.5 DC approximation

“DC approximation” is a name given to a collection of assumptions/approximations, described below. The name ‘DC’ refers to the approximation that the network is decoupled. Unlike the abbreviation might suggest, the power grid is still modelled as an AC network.

Scott1974  
for the origin of the DC approximation

Compare the following with Definitions 5.1.1 and 5.2.1.

**Definition 5.5.1.** Suppose  $((\mathcal{N}, \mathcal{L}), \mathbf{C}, \boldsymbol{\eta})$  is an  $(n, m)$ -grid structure, with a grid state  $(\mathbf{S}, \mathbf{V}, \mathbf{I})$ .

- If  $\boldsymbol{\eta} \in i\mathbb{R}^m \subseteq \mathbb{C}^m$  (i.e.  $\boldsymbol{\eta}$  has purely imaginary values) then the grid structure *satisfies the DC approximation*.<sup>7</sup>
- If  $\mathbf{S} \in \mathbb{R}^n \subseteq \mathbb{C}^n$  then the grid state *satisfies the DC approximation*. (Note that  $\mathbf{V}$  and  $\mathbf{I}$  need not be real-valued.)
- If  $\mathbf{V} \in \mathbb{T}^n \cdot V_{op} \subseteq \mathbb{C}^n$  (i.e.  $|V_i| = V_{op}$  for each node  $i$ ) for some *operating voltage*  $V_{op} \in \mathbb{R}_{\geq 0}$ , then the grid state admits a *flat profile*.

In the special case  $V_{op} = 1$ , the grid state admits a *normalised profile*.

By replacing the exp function in (5.1) by  $z \mapsto 1 + z$  (the first two terms of the Maclaurin series of exp) we get the *approximate node flow equation*. These two conditions are different, but as we will later see, similar for networks with small phase shifts. Compare the following with Definition 5.3.1 and (5.1).

**Definition 5.5.2.** Given an  $(n, m)$ -grid structure  $((\mathcal{N}, \mathcal{L}), \mathbf{C}, \boldsymbol{\eta})$ , a grid state  $(\mathbf{S}, \mathbf{V}, \mathbf{I})$  is *DC-valid* if it satisfies the *KVL-Ohm equality*:

$$\mathbf{I} = i \operatorname{diag}(i\boldsymbol{\eta})\mathbf{C}\mathbf{V} \quad (\text{KVL-Ohm})$$

and each node  $i$  satisfies the *approximate node flow equation*:

$$S_i = i \sum_{j=1}^n L_{i,j}^* |V_i| |V_j| (1 + i(\theta_i - \theta_j)) \quad \text{for each } i \in [n]. \quad (5.5)$$

**Theorem 5.5.3.** Suppose that a grid structure and state satisfy the DC approximation and that the state admits a flat, normalised profile. Then the approximated node flow equation is linear and real:

$$\mathbf{S} = \mathbf{L}\boldsymbol{\theta}. \quad (5.6)$$

*Proof.* For each node  $i$ , we have:

$$\begin{aligned} S_i &= i \sum_{j=1}^n L_{i,j}^* |V_i| |V_j| (1 + i(\theta_i - \theta_j)) \\ &= i \sum_{j=1}^n L_{i,j} |V_i| |V_j| - \sum_{j=1}^n L_{i,j} |V_i| |V_j| (\theta_i - \theta_j) \end{aligned}$$

<sup>7</sup>In Nesti et al., we have  $\beta = i\boldsymbol{\eta}$ . Transmission line impedance ( $Z = R + iX$ ) is dominated by inductance, which is positive reactance ( $X$ ). Resistance ( $R$ ) is always positive for passive components. Therefore,  $Z$  lies in the top-right quadrant of  $\mathbb{C}$ . Then the admittance,  $Y = 1/Z = G + iB$ , lies in the bottom-right quadrant of  $\mathbb{C}$ . In the DC approximation, line conductance ( $G$ ) is neglected, so ( $Y = iB$  with  $B < 0$ ). Therefore,  $\beta_k = i\eta_k = iY = -B > 0$  is the *susceptance of line  $k$ , with reversed sign*.

physics:  
conductance  
is neglected

physics:  
only phase  
shifts are  
considered,  
unit is p.u.  
instead of  
Volts

hyp: a (DC-  
?)valid state  
can only  
exist if the  
structure  
and state  
both sat-  
isfy the DC  
approx (oth-  
erwise no  
line drop  
can occur?)

discuss line  
drop

this is also  
approx-  
imated:  $\mathbf{C}\mathbf{V}$   
is linearised.



If we assume a DC state ( $S_i \in \mathbb{R}$ ):

$$\begin{aligned}
&= - \sum_{j=1}^n L_{i,j} |V_i| |V_j| (\theta_i - \theta_j) \\
&= - \sum_{j=1}^n L_{i,j} |V_i| |V_j| \theta_i + \sum_{j=1}^n L_{i,j} |V_i| |V_j| \theta_j \\
&= -\theta_i |V_i| \sum_{j=1}^n L_{i,j} |V_j| + |V_i| \sum_{j=1}^n L_{i,j} |V_j| \theta_j
\end{aligned}$$

If we assume a flat profile ( $|V_i| = |V_j| = V_{op}$  for every  $i, j \in [n]$ ):

$$= -\theta_i V_{op}^2 \sum_{j=1}^n L_{i,j} + V_{op}^2 \sum_{j=1}^n L_{i,j} \theta_j$$

The rows of  $L$  add up to 0:

$$\begin{aligned}
&= V_{op}^2 \sum_{j=1}^n L_{i,j} \theta_j \\
&= V_{op}^2 (\mathbf{L}\boldsymbol{\theta})_i
\end{aligned}$$

If we assume  $\mathbf{V}$  to be normalised (if  $V$  is measured in p.u., instead of Volts):

$$= (\mathbf{L}\boldsymbol{\theta})_i$$

and we find:

$$\mathbf{S} = \mathbf{L}\boldsymbol{\theta}$$



Appendix: give a direct formula for  $\mathbf{L}$

compute  $\mathbf{L}$  for the example networks

give an alternative interpretation of  $\mathbf{L}$  or  $\mathbf{L}$ : discrete laplacian

discuss the kernel of  $\mathbf{L}$ : it should follow from graph theoretical arguments that the kernel is spanned by  $(1, 1, \dots, 1)^T$ , such that the nullity of  $\mathbf{L}$  is 1. This corresponds to the fact that phase angle is a relative quantity. (The state remains (DC-)valid when increasing the phase angle at each node by the same amount. (If  $\mathbf{S} = \mathbf{L}\boldsymbol{\theta}$  and  $\boldsymbol{\theta}_0 \in \ker \mathbf{L}$ , then  $\mathbf{S} = \mathbf{L}(\boldsymbol{\theta} + \boldsymbol{\theta}_0)$ .)

There are two paths to take after this point:

1: Fix the phase angle of the slack bus (to 0), which corresponds to taking the  $n - 1 \times n - 1$  submatrix of  $\mathbf{L}$ , I think. **This is the approach of PyPSA, which might explain small differences in line flow.**

2: Leave  $\mathbf{L}$  as-is, and consider the *Moore-Penrose pseudo-inverse* of  $\mathbf{L}$ . This is the approach of Nesti et al., which they attribute to 'distributive slack': not fixing a single slack bus.

### 5.5.1 Usefulness

Real transmission networks do not satisfy the DC approximation and, in general, a DC-valid state is not (physically) valid. Yet, using these two approximations has one important property: the approximated node flow equation becomes *linear*. This has a number of advantages:

- Solving the Power Flow problem (i.e. computing line flows induced by a power injection vector) becomes trivial. As we will see in Section 5.6,

ref

ugh

- A linear power flow is crucial for the study of stochastic power injections, since it can be used to transform a probability distribution (like a multivariate normal distribution) without losing its structure.

be specific

### 5.5.2 Accuracy

The DC approximation is a useful tool for understanding the complex nature of transmission networks. Therefore, it is crucial to verify that the DC approximation is, in fact, a good approximation, when real-world networks are studied. More precisely, one should ask:

1. How close is a DC-valid state to being valid? More precisely, when the approximate node flow equation (5.5) holds, what is the mismatch between the left hand and right hand side of the node flow equation (5.1)?
2. How close are real-world grid structures to satisfying the DC approximation?

The first question is answered in Proposition 5.5.5, where an upper bound is derived for the power mismatch. It shows that the mismatch is bounded by the *squares* of local differences in phase angles (i.e.  $\theta_i - \theta_j$  for line  $(i, j)$ ). Purchala et al. (2005) have shown that in the Belgian transmission network, all phase differences are below  $7^\circ$ , and 94% of lines have a phase difference below  $2^\circ$ .

europe

The second question

SciGRID

acc of DC approx struc vs acc of DC valid state

Purchala

**Lemma 5.5.4.** *There exists  $K \in \mathbb{R}_{>0}$  such that*

$$|\exp ix - (1 + ix)| = K|x|^2 \quad \text{for every } -2\pi \leq x \leq 2\pi.$$

literature:  
Purchala  
et al. (2005);  
Overbye  
et al. (2004)

*Proof.* **A proof using complex analysis.**<sup>8</sup> The complex (entire) function  $z \mapsto \exp z$  is defined by the power series

$$z \mapsto \sum_{k=0}^{\infty} \frac{z^k}{k!} = 1 + z + z^2 \left( \frac{z^0}{2!} + \frac{z^1}{3!} + \dots \right)$$

Move to ap-  
pendix?

Find an up-  
per bound  
for  $K$ ,  
 $K = 0.5$   
works

<sup>8</sup>For an introduction, see Garling (2014).

which has infinite radius of convergence, and is continuous on  $\mathbb{C}$ .


0<sup>0</sup>

The functions  $z \mapsto \frac{1}{z^2}$ ,  $z \mapsto \exp z$  and  $z \mapsto 1 + z$  are all holomorphic on  $\mathbb{C}^* = \mathbb{C} \setminus \{0\}$ , and so the function

$$g : \mathbb{C}^* \rightarrow \mathbb{C} \quad g : z \mapsto \frac{1}{z^2}(\exp z - (1 + z)) \quad (5.7)$$

is holomorphic on  $\mathbb{C}^*$ , with a removable singularity at 0. The (unique) extension of  $g$  to  $\mathbb{C}$  is an entire function, and by construction:

$$\exp z = 1 + z + z^2 g(z) \quad \text{for each } z \in \mathbb{C}.$$

Since  $g$  is entire, it is continuous on  $\mathbb{C}$ .  $I = [-i2\pi, i2\pi]$  is a compact subset of  $\mathbb{C}$ , so  $g$  is bounded on  $I$ , proving the result. 

**Proposition 5.5.5.** *Suppose  $((\mathcal{N}, \mathcal{L}), \mathbf{C}, \boldsymbol{\eta})$  is an  $(n, m)$ -grid structure, with a state  $(\mathbf{S}, \mathbf{V}, \mathbf{I})$  that admits a flat profile with operating voltage  $V_{op}$ .*

*If the state is DC-valid, then there exists  $K \in \mathbb{R}_{\geq 0}$  such that for each node  $i$ :*

$$\begin{aligned} \left| S_i - i \sum_{j=1}^n L_{i,j}^* |V_i| |V_j| e^{i(\theta_i - \theta_j)} \right| &\leq K V_{op}^2 \sum_{j=1}^n |L_{i,j}| (\theta_i - \theta_j)^2 \\ &\leq K V_{op}^2 \|\boldsymbol{\eta}\|_{\infty} \|\mathbf{C}\boldsymbol{\theta}\|_2^2. \end{aligned}$$

*Remark.* This result states that if the grid state is *DC-valid*, and the power angles (i.e.  $\theta_i - \theta_j$  for line  $(i, j)$ ) are low, then the state is *close* to also being *valid*.

Quantitatively, it tells us that for a given node  $i$ , the 'error' resulting from using the approximate node flow equation (5.5) is proportional to the *squares* of phase angles of lines that connect to  $i$ .

*Proof.* Suppose  $i \in [n]$ .

Choose a  $K \in \mathbb{R}_{\geq 0}$  for which Lemma 5.5.4 holds. The state is DC-valid, so we can

A more important result would be an upper limit for the error in *line flow*, instead of the error in *node flow*

this follows from the proof, not the statement itself

substitute (5.5) for  $S_i$ :

$$\begin{aligned}
& \left| S_i - \sum_{j=1}^n M_{i,j}^* |V_i| |V_j| e^{i(\theta_i - \theta_j)} \right| \\
&= \left| i \sum_{j=1}^n L_{i,j}^* |V_i| |V_j| (1 + i(\theta_i - \theta_j)) - i \sum_{j=1}^n L_{i,j}^* |V_i| |V_j| e^{i(\theta_i - \theta_j)} \right| \\
&= V_{op}^2 \left| \sum_{j=1}^n L_{i,j}^* \left( e^{i(\theta_i - \theta_j)} - (1 + i(\theta_i - \theta_j)) \right) \right| \\
&\leq V_{op}^2 \sum_{j=1}^n |L_{i,j}| \left| e^{i(\theta_i - \theta_j)} - (1 + i(\theta_i - \theta_j)) \right| \quad (\text{triangle inequality}) \\
&\leq KV_{op}^2 \sum_{j=1}^n |L_{i,j}| (\theta_i - \theta_j)^2 \quad (\text{Lemma 5.5.4}) \\
&= KV_{op}^2 \left[ \sum_{j=i} |L_{i,j}| (\theta_i - \theta_j)^2 + \sum_{\substack{j \neq i \\ i,j \text{ connected}}} |L_{i,j}| (\theta_i - \theta_j)^2 + \sum_{\substack{j \neq i \\ i,j \text{ not connected}}} |L_{i,j}| (\theta_i - \theta_j)^2 \right] \\
&= KV_{op}^2 \left[ |L_{i,i}| (\theta_i - \theta_i)^2 + \sum_{\substack{j \neq i \\ i,j \text{ connected}}} |L_{i,j}| (\theta_i - \theta_j)^2 + \sum_{\substack{j \neq i \\ i,j \text{ not connected}}} 0 \cdot (\theta_i - \theta_j)^2 \right] \\
&= KV_{op}^2 \sum_{\substack{j \neq i \\ i,j \text{ connected}}} |L_{i,j}| (\theta_i - \theta_j)^2 \\
&\leq KV_{op}^2 \sum_{\mathcal{L}_k = (a,b) \in \mathcal{L}} |L_{a,b}| (\theta_a - \theta_b)^2 \\
&= KV_{op}^2 \sum_{\mathcal{L}_k = (a,b) \in \mathcal{L}} |\eta_k| (C\theta)_k^2 \\
&= KV_{op}^2 \|\boldsymbol{\eta} * \mathbf{C}\boldsymbol{\theta} * \mathbf{C}\boldsymbol{\theta}\|_1 \quad (\text{in } \ell^1) \\
&\leq KV_{op}^2 \|\boldsymbol{\eta}\|_\infty \|\mathbf{C}\boldsymbol{\theta} * \mathbf{C}\boldsymbol{\theta}\|_1 \quad (\text{Hölder's inequality}) \\
&= KV_{op}^2 \|\boldsymbol{\eta}\|_\infty \|\mathbf{C}\boldsymbol{\theta}\|_2^2
\end{aligned}$$



Discuss the PDEs used for computing the PF?

## 5.6 Linear Power Flow

Physically, power does not actually flow. (Although *energy* does). A better term would be: *flow power*, since a high power flow from A to B is actually a *powerful flow of energy* from A to B.

In the context of line overloads, we are only interested in line *current*, which can be seen as proportional to the amount of power being transmitted by the line. (Again, power is not a physical quantity that can be transmitted.) In a flat, normalised profile, power flow and line current are identical. To follow general convention, we will talk about power flow instead of line current. For example, line ratings are often given in Watts, not Amperes. (Even though the amount energy dissipated by a line,  $I^2R$ , depends only on line current. At a nearly constant operating voltage, however, these quantities are proportional to each other.)

DC approx, flat, normalised state and DC valid:

pseudoinverse:

$$\mathbf{p} = \mathbf{L}\boldsymbol{\theta}$$

so there exists  $\mathbf{L}^+$  such that

$$\boldsymbol{\theta} = \mathbf{L}^+\mathbf{p}$$

this is the moore-penrose pseudo-inverse,

My DC approximated KVL-Ohm is incorrect, it should be:  $\mathbf{I} = i \text{diag}(i\boldsymbol{\eta})\mathbf{C}\boldsymbol{\theta}V_{op}$ .

$$\hat{\mathbf{f}} = -iV_{op}\mathbf{I} = -iV_{op}^2 i \text{diag}(i\boldsymbol{\eta})\mathbf{C}\boldsymbol{\theta} = \text{diag}(i\boldsymbol{\eta})\mathbf{C}\mathbf{L}^+\mathbf{p}.$$

(We assumed a normalised profile, so  $V_{op} = 1$ .)

If the line thresholds are  $\mathbf{W} = (W_1, \dots, W_m)^T \in \mathbb{R}^m$ , then we can define the *normalised line flow* as:

$$\mathbf{f} = \text{diag}(\mathbf{W})^{-1}\hat{\mathbf{f}}$$

and we find:

$$\mathbf{f} = \mathbf{F}\mathbf{p} \quad (\text{LPF})$$

where  $\mathbf{F} = \text{diag}(\mathbf{W})^{-1} \text{diag}(i\boldsymbol{\eta})\mathbf{C}\mathbf{L}^+$

Dit is

This is a linear transformation from a power injection vector  $\mathbf{p}$  to the normalised line flow  $\mathbf{f}$  that induces it.

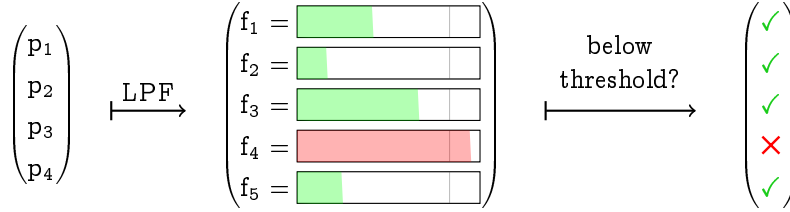
$\mathbf{F}$  is not the unique transformation with this property (otherwise  $\mathbf{F}$  would be square and non-singular). Does  $\mathbf{F}$  minimise  $\|\mathbf{f}\|$ ?  $\mathbf{F}$

Leg het verband tussen de LPF en het hoofdstuk over grafen: de af

line drop:  
(real) power  
flowing out  
of a node  
is slightly  
more than  
power

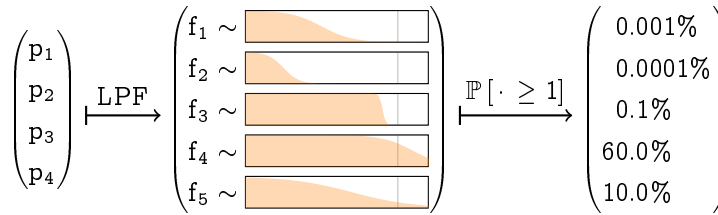
## 5.7 Stochastic power injections

Using the linear transformation  $\mathbf{F}$  that we just derived, we can compute the normalised line flow that a *zero-sum* power injection  $\mathbf{p}$  induces. This is a useful result: for example, one could check whether a generator configuration is *admissible* by writing down the injection  $\mathbf{p}$  associated to this configuration, and checking that no value of  $\mathbf{F}\mathbf{p}$  is greater than 1. (Since we *normalised* the line flows, each line has unit 'threshold'.)



grafiekjes  
zijn van  $|f|$ ,  
niet  $f$ .

Things get even more interesting when  $\mathbf{p}$  is a *stochastic variable*. In this case,  $\mathbf{f}$  is also a stochastic variable! In fact, given a probability distribution function for  $\mathbf{p}$ , we can use  $\mathbf{F}$  to compute the *probability distribution function of  $\mathbf{f}$* . Using this probability distribution, we can now answer questions such as: “What is the probability that line  $i$  overloads?” ( $\mathbb{P}[f_i \geq 1]$ ) Or: “What is the probability that line  $i$  overloads, given that line  $j$  is operating at 95% capacity?” ( $\mathbb{P}[f_i \geq 1 \mid f_j = 0.95]$ ).



grafiekjes  
zijn van  $|f|$ ,  
niet  $f$ .

### 5.7.1 Normally distributed power injection

Following Nesi et al. (2018a), we model  $\mathbf{p}$  to be *multivariate normally distributed*:

$$\mathbf{p} \sim \mathcal{N}(\boldsymbol{\mu}_p, \boldsymbol{\Sigma}_p)$$

where  $\boldsymbol{\mu}_p$  is the mean power injection, which is the sum of deterministic generation and expected stochastic generation, minus the load.  $\boldsymbol{\Sigma}_p$  is the *power injection correlation matrix*, which can be estimated from historical generation series. When power injection at different nodes is correlated (because of correlated weather), this matrix is non-diagonal.

Because  $\mathbf{F}$  is a linear transformation, the vector of line flows  $\mathbf{f}$  is (multivariate) Gaussian distributed (Theorem 1.4.6), and its distribution is given by

$$\mathbf{f} \sim \mathcal{N}(\boldsymbol{\mu}_f, \boldsymbol{\Sigma}_f), \quad \text{where} \quad \boldsymbol{\mu}_f = \mathbf{F}\boldsymbol{\mu}_p \quad \text{and} \quad \boldsymbol{\Sigma}_f = \mathbf{F}\boldsymbol{\Sigma}_p\mathbf{F}^*. \quad (5.8)$$

For realistic networks we have  $m > n$ , which means that  $\mathbf{F}$  is not surjective. Then  $\boldsymbol{\Sigma}_f$  is not injective, meaning that  $\mathbf{f}$  is Gaussian, but not normally distributed (Theorem 1.4.5).

### 5.7.2 Overload probabilities

For a line  $l$ , the probability distribution of the current through that line is simply the marginal distribution  $f_l$ . Therefore, the probability of an emergent failure of line  $l$  is given by:<sup>9</sup>

$$\mathbb{P}[|f_l| \geq 1] = \mathbb{P}[f_l \leq -1] + \mathbb{P}[f_l \geq 1]$$

From Theorem 1.4.7 it follows that  $f_l \sim \mathcal{N}(\mu_{fl}, \Sigma_{flu})$ , and  $\mathbb{P}[|f_l| \geq 1]$  can now be computed using standard techniques.

The probability of *any* emergent failure is  $\mathbb{P}[\exists_{l \in [m]} |f_l| \geq 1]$ , which can be approximated by an upper and lower bound:

Or estimated using the LDP

$$\min_{l \in [m]} \mathbb{P}[|f_l| \geq 1] \leq \mathbb{P}[\exists_{l \in [m]} |f_l| \geq 1] \leq \sum_{l \in [m]} \mathbb{P}[|f_l| \geq 1].$$

Trivially, the most likely line flow, given that any emergent failure occurred, coincides with most likely line flow, given that the most vulnerable line failed.

### 5.7.3 Most likely power injection

Now that we have identified the most vulnerable lines in the network, we naturally want to simulate the effect that the failure of one of these lines will have. When we remove the line from our model, we get a new LPF matrix, which can be used to check the currents through all other lines, after the initial failure. But what power injection should be used? Because we are studying the *hypothetical* failure of a line, we do not yet know the exact power injection that caused it.

The classical approach is to use the nominal power injection,  $\mu_p$ . This is exactly what we would do when studying regular line failures (caused by a fallen tree, for example). In our case, however, we assumed that the line failed because of an *overload*, which tells us that the power injection must have deviated from its nominal value.

Because we have estimated a probability distribution for  $p$ , we can find *the most likely power injection, given that line  $l$  overloaded*. We can compute this injection explicitly, leveraging the fact that the LPF map is linear.

**Theorem 5.7.1.** *Suppose a grid with LPF  $F$  has a  $\mathcal{N}(\mu_p, \Sigma_p)$ -distributed power injection  $p$ . The most likely power injection  $\tilde{p}^{(l)}$ , given the emergent failure of a line  $l$ , is uniquely given by*

$$\tilde{p}^{(l)} = \mu_p + \frac{\text{sign}(\mu_{fl}) - \mu_{fl}}{\Sigma_{flu}} \Sigma_p F^* e_l \quad (5.9)$$

when  $\mu_{fl} \neq 0$ . Otherwise, there are two injections that maximise the conditional probability of  $p$ , which are given by

$$\tilde{p}^{(l,+)} = \mu_p + \frac{1}{\Sigma_{flu}} \Sigma_p F^* e_l \quad \text{and} \quad \tilde{p}^{(l,-)} = \mu_p - \frac{1}{\Sigma_{flu}} \Sigma_p F^* e_l.$$

<sup>9</sup>Remember that the *sign* of  $f_l$  corresponds to the *direction* of current through the line. The line orientations were chosen arbitrarily, and only have meaning in our bookkeeping.

*Proof.* The set of power injections associated with the failure event of line  $l$  is a union of two parallel *planes* in  $\mathbb{R}^n$ . Indeed, the condition  $f_l = 1$  can be written as:

$$f_l = 1 \iff (\mathbf{F}\mathbf{p})_l = 1 \iff \mathbf{e}_l^* \mathbf{F}\mathbf{p} = 1 \iff \langle \mathbf{F}^* \mathbf{e}_l, \mathbf{p} \rangle = 1$$

which is the equation defining the plane with pillar  $\mathbf{F}^* \mathbf{e}_l$ . Similarly, the condition  $f_l = -1$  is satisfied if and only if  $\mathbf{p}$  is contained in the plane with pillar  $-\mathbf{F}^* \mathbf{e}_l$ .


We can now apply Theorem 1.4.12 to each pillar to find the mode of  $\mathbf{p}$ , given  $f_l = 1$ , or  $f_l = -1$ , respectively:

$$\begin{aligned} \tilde{\mathbf{p}}^{(l,+)} &= \mu_{\mathbf{p}} + \frac{1 - \langle \mu_{\mathbf{p}}, \mathbf{F}^* \mathbf{e}_l \rangle}{\langle \Sigma_{\mathbf{p}} \mathbf{F}^* \mathbf{e}_l, \mathbf{F}^* \mathbf{e}_l \rangle} \Sigma_{\mathbf{p}} \mathbf{F}^* \mathbf{e}_l \\ &= \mu_{\mathbf{p}} + \frac{1 - \langle \mathbf{F} \mu_{\mathbf{p}}, \mathbf{e}_l \rangle}{\langle \mathbf{F} \Sigma_{\mathbf{p}} \mathbf{F}^* \mathbf{e}_l, \mathbf{e}_l \rangle} \Sigma_{\mathbf{p}} \mathbf{F}^* \mathbf{e}_l \quad (\mathbf{F}^* \text{ is the adjoint of } \mathbf{F}) \\ &= \mu_{\mathbf{p}} + \frac{1 - \langle \mu_{\mathbf{f}}, \mathbf{e}_l \rangle}{\langle \Sigma_{\mathbf{f}} \mathbf{e}_l, \mathbf{e}_l \rangle} \Sigma_{\mathbf{p}} \mathbf{F}^* \mathbf{e}_l \\ &= \mu_{\mathbf{p}} + \frac{1 - \mu_{\mathbf{f}l}}{\Sigma_{\mathbf{f}ll}} \Sigma_{\mathbf{p}} \mathbf{F}^* \mathbf{e}_l \end{aligned} \tag{5.10}$$

$$\begin{aligned} \tilde{\mathbf{p}}^{(l,-)} &= \mu_{\mathbf{p}} - \frac{1 - \langle \mu_{\mathbf{p}}, -\mathbf{F}^* \mathbf{e}_l \rangle}{\langle -\Sigma_{\mathbf{p}} \mathbf{F}^* \mathbf{e}_l, -\mathbf{F}^* \mathbf{e}_l \rangle} \Sigma_{\mathbf{p}} \mathbf{F}^* \mathbf{e}_l \\ &= \mu_{\mathbf{p}} + \frac{-1 - \langle \mu_{\mathbf{p}}, \mathbf{F}^* \mathbf{e}_l \rangle}{\langle \Sigma_{\mathbf{p}} \mathbf{F}^* \mathbf{e}_l, \mathbf{F}^* \mathbf{e}_l \rangle} \Sigma_{\mathbf{p}} \mathbf{F}^* \mathbf{e}_l \\ &\vdots \\ &= \mu_{\mathbf{p}} + \frac{-1 - \mu_{\mathbf{f}l}}{\Sigma_{\mathbf{f}ll}} \Sigma_{\mathbf{p}} \mathbf{F}^* \mathbf{e}_l. \end{aligned} \tag{5.11}$$

By symmetry of the marginal distribution of  $f_l$ , it follows that in the unlikely case where  $\mu_{\mathbf{f}l}$  is zero, the line current is equally likely to deviate to the left as it is to deviate to the right, and both cases come with a different power injection. When  $\mu_{\mathbf{f}l}$  is non-zero, one of the two cases is more likely.

$$\begin{aligned} \mu_{\mathbf{f}l} > 0 &\iff \tilde{\mathbf{p}}^{(l,+)} \text{ is the most probable injection,} \\ \mu_{\mathbf{f}l} = 0 &\iff \tilde{\mathbf{p}}^{(l,+)} \text{ and } \tilde{\mathbf{p}}^{(l,-)} \text{ are the two most probable injections,} \\ \mu_{\mathbf{f}l} < 0 &\iff \tilde{\mathbf{p}}^{(l,-)} \text{ is the most probable injection.} \end{aligned}$$

When  $\mu_{\mathbf{f}l} \neq 0$ , we can use the sign function to combine Equations (5.10) and (5.11) into one, which gives the desired expression. 

Large dev: in het limiet  $\epsilon \rightarrow 0$  valt de verwachtingswaarde van  $\mathbf{p}$ , gegeven emergent failure  $l$ , samen met de zojuist gegeven mode.

## 5.8 Redistribution of flow

In the previous section, we studied normally distributed power injections, and we can now discover which lines are likely to fail, and what power injection was the most likely



cause. The next step is to study the *redistribution of flow*: when overloaded lines are switched off (which happens almost instantly), the remaining lines in the network will have to take over their function, because *the power injection remains unchanged after a line outage*. In the simplest case of two parallel lines that connect two otherwise unconnected grids (say, a geographical island connected to the mainland via two cables), the failure of one line will force the other line to carry its original current, plus the current that would normally flow through the failed line.

Except for special cases like these, this *redistributed flow* is, in general, hard to compute without the tools developed in this section. The general case not only consists of all possible line failures, we also want to study all *possible combinations* of line failures.

We will discuss two methods to solve this problem: the Direct and the Optimised methods. The first method simply considers the graph obtained by removing the failed lines from the network, and then recalculates (LPF) for the network. Calculating the Moore-Penrose inverse of  $\mathbf{L}$  is computationally expensive<sup>10</sup>, and every combination of line failures requires this calculation.<sup>11</sup> A second method, first introduced by ?, utilises the LPF of the original network to derive the redistribution of flow. This Optimised method is computationally less expensive, and provides additional insight into the effect of line outages, that would not be obtained when discarding the original network.

LODF matrix

### 5.8.1 Direct method

Eigenlijk is deze methode net al verteld. Misschien is dit een goede plek voor power islands?

For the Direct method, we simply recompute the LPF for the perturbed network. To avoid reducing the dimension  $m$ , and recalculating  $\mathbf{C}$ , we set the admittance of each failed line to zero.

More formally, suppose  $((\mathcal{N}, \mathcal{L}), \mathbf{C}, \boldsymbol{\eta})$  is an  $(n, m)$ -grid structure with  $\mathcal{Z} \subseteq [m]$  a collection of  $v \in [m]$  lines that fail. For an injection  $\mathbf{p} \in \mathbb{R}^n$ , the line flow

the line flows *before* the failures of  $\mathcal{Z}$  is given by:

$$\mathbf{f}^{\mathcal{Z}} = \text{diag}(i\boldsymbol{\eta})\mathbf{C}(\mathbf{C}^* \text{diag}(i\boldsymbol{\eta})\mathbf{C})^+ \mathbf{p} \quad (5.12)$$

(by definition of  $\mathbf{F}$ ) and the line flows *after* the failures are given by:

$$\mathbf{f}^{\mathcal{Z}} = \text{diag}(i\boldsymbol{\eta})\mathbf{C}(\mathbf{C}^* \text{diag}(i\boldsymbol{\eta})\mathbf{I}_{[m] \setminus \mathcal{Z}}\mathbf{C})^+ \mathbf{p}, \quad (5.13)$$

where  $\mathbf{I}_{[m] \setminus \mathcal{Z}}$  is the identity matrix, with diagonal entries set to zero for line numbers contained in  $\mathcal{Z}$ . By taking the product  $\text{diag}(i\boldsymbol{\eta})\mathbf{I}_{[m] \setminus \mathcal{Z}}$ , we are essentially setting the admittance of failed lines to zero, which corresponds physically to a circuit break.

<sup>10</sup>Scientific computing libraries generally calculate  $\mathbf{L}^+$  using the Singular Value Decomposition of  $\mathbf{L}$ .

<sup>11</sup>Calculating the LPF of the SciGrid network ( $n = 489$ ,  $m = 895$ ) takes approximately 700 ms, excluding the additional overhead of copying the unperturbed network.

### 5.8.2 Optimised method

**Theorem 5.8.1.** *Suppose  $((\mathcal{N}, \mathcal{L}), \mathbf{C}, \boldsymbol{\eta})$  is an  $(n, m)$ -grid structure, with  $LPF \mathbf{F}$ . Suppose that  $\mathcal{Z} \subseteq [m]$  is a collection of  $v \in [m]$  lines that fail. For a given injection  $\mathbf{p} \in \mathbb{R}^n$ , the line flows before the failures of  $\mathcal{Z}$  are given by:*

$$\mathbf{f} = \mathbf{F}\mathbf{p} \quad (5.14)$$

$$(5.15)$$

and the line flows after the failures are given by:

$$\mathbf{f}^{\mathcal{Z}} = \mathbf{f} - \mathbf{M}\mathbf{N}(\mathbf{N}^*\mathbf{M}\mathbf{N})^+ \mathbf{N}^*\mathbf{f} \quad (5.16)$$

where  $\mathbf{M} = \mathbf{F}\mathbf{C}^* - \mathbf{I} \in \mathbb{R}^{m \times m}$  and  $\mathbf{N} = (\mathbf{e}_{\mathcal{Z}_1} \cdots \mathbf{e}_{\mathcal{Z}_v}) \in \mathbb{R}^{m \times v}$ , the matrix that is zero everywhere, except for the entries  $(\mathcal{Z}_i, i)$  (for  $i \in [v]$ ), where it has value 1.

*Remark.* This expression for  $\mathbf{f}^{\mathcal{Z}}$  also contains a pseudo-inverse, which might not look computationally advantageous, compared to the Direct method. Note, however, that right multiplying by  $\mathbf{N}$  corresponds to taking the submatrix of column numbers  $\mathcal{Z}_1$  through  $\mathcal{Z}_v$ , and left multiplying by  $\mathbf{N}^*$  gives the submatrix of row numbers in  $\mathcal{Z}$ . This means that  $\mathbf{M}$  only needs to be computed once, after which most matrix multiplications in (5.16) can be done by *indexing appropriately*, for any combination of line failures. Additionally, if the number of failed lines is small, the product  $\mathbf{N}^*\mathbf{M}\mathbf{N}$  will be a small matrix, drastically improving performance. Lastly, this expression only requires (pseudo-)solving the system of equations  $(\mathbf{N}^*\mathbf{M}\mathbf{N})\boldsymbol{\alpha} = \mathbf{N}^*\mathbf{f}$ , which can be done more efficiently than computing the full pseudo-inverse. (The same optimisation can be also applied to the Direct method.)

Several proofs to this theorem exist. The first proof, by ?, iterates over the failed lines, proving the result by natural induction. (?) provide two additional proofs, which follow from a careful analysis of the Direct method, where they *remove the rows of  $\mathbf{C}$*  that correspond to failed lines. An entirely different, fourth proof, due to ?, uses the formalism of *graph cycles*, which form a basis for  $\ker \mathbf{C}^*$ . Their article is truly fascinating, as it explores how flow redistributions are composed of loop flows. Additionally, they derive a more general result, where the grid perturbation is expressed as a *change in line admittances  $\boldsymbol{\eta}$* .<sup>12</sup> Taking the limit  $\eta_l \rightarrow 0$  then corresponds to the removal of the line.

Before providing this fourth proof, we will try to deduce the result from intuitive reasoning, to better understand the found expression.

*Intuitive argument.* Both  $\mathbf{f}$  and  $\mathbf{f}^{\mathcal{Z}}$  are induced by the same power injection, i.e.  $\mathbf{C}^*\mathbf{f} = \mathbf{C}^*\mathbf{f}^{\mathcal{Z}} = \mathbf{p}$ . This means that the difference between the two, which is the change in flow right after the line failures, is an *element of the kernel of  $\mathbf{C}^*$* . We denote this difference by  $\Delta\mathbf{f} := \mathbf{f}^{\mathcal{Z}} - \mathbf{f}$ .

For each  $l \in \mathcal{Z}$ , the current through line  $l$  must become zero. This imposes the condition

$$\Delta f_l = f_l^{\mathcal{Z}} - f_l = -f_l, \quad (5.17)$$

<sup>12</sup>Some transmission networks deploy adjustable inductors that clamp onto transmission lines, to *steer* the flow of current, making this generalisation especially relevant.

or more compactly,

$$\mathbf{N}^* \Delta \mathbf{f} = -\mathbf{N}^* \mathbf{f}. \quad (5.18)$$

Let us first consider the case of a single failure:  $\mathcal{Z} = \{l\}$ , that does not cause the network to become disconnected. We are looking for a  $\Delta \mathbf{f} \in \ker \mathbf{C}^*$ , under the condition that  $f_l^{\mathcal{Z}} = -f_l$ . The first choice that might come to mind is to fix a basis of  $\ker \mathbf{C}^*$  consisting of *unit loop flows* in the graph. We can pick a unit loop flow that is non-zero at  $l$ , and scale by  $\pm f_l$  to find the desired flow difference.

Although this does satisfy the condition at  $l$ , it is in general not the flow that will be *induced* in the perturbed network, which is uniquely determined by power flow physics. There are many linear combinations of unit loop flows that satisfy the condition at  $l$ , one of which is the correct one.

Suppose that the network is unused ( $\mathbf{p} = \mathbf{0}$ ), and we *force* a current of 1 through line  $l$ , and fix all other line currents to 0. This line flow vector is given by  $\mathbf{e}_l$ . The result of this flow will be a power injection which remains zero everywhere, except at the two nodes that  $\mathcal{L}_l = (i, j)$  connects. This power injection is given by  $\mathbf{C}^* \mathbf{e}_l$ .

On the other hand, if we were to apply the injection  $\mathbf{C}^* \mathbf{e}_l$  to the network, allowing current to flow naturally, we would find the vector of line currents  $\mathbf{F} \mathbf{C}^* \mathbf{e}_l$ , which in general does not equal  $\mathbf{e}_l$ ! Of course, the natural line flow in  $l$  will still be relatively large, but some power will be transmitted along different routes. For example, in a circular network of four buses and four lines of equal admittance, with  $l = 1$ , we find<sup>13</sup>

$$\mathbf{F} \mathbf{C}^* \mathbf{e}_1 = \begin{pmatrix} 0.75 \\ -0.25 \\ -0.25 \\ -0.25 \end{pmatrix}, \text{ with difference } \mathbf{F} \mathbf{C}^* \mathbf{e}_1 - \mathbf{e}_1 = \begin{pmatrix} -0.25 \\ -0.25 \\ -0.25 \\ -0.25 \end{pmatrix}.$$

Because  $\mathbf{F}$  is the right-inverse of  $\mathbf{C}^*$ , we find that  $\mathbf{C}^* (\mathbf{F} \mathbf{C}^* \mathbf{e}_l) = \mathbf{C}^* \mathbf{e}_l$ , which means that the *difference between a natural flow and a forced flow*,  $\mathbf{F} \mathbf{C}^* \mathbf{e}_l - \mathbf{e}_l$ , is an element of the kernel of  $\mathbf{C}^*$ .

We have not yet satisfied the condition (5.18). Given a power injection  $\mathbf{p}$  and unperturbed flow  $\mathbf{f} = \mathbf{F} \mathbf{p}$ , we can *scale* the above difference with some  $\alpha \in \mathbb{R}$ :

$$\Delta \mathbf{f} = (\mathbf{F} \mathbf{C}^* \mathbf{e}_l - \mathbf{e}_l) \alpha$$

with  $\alpha$  such that

$$\Delta f_l = -f_l$$

is satisfied. If the network remains connected,  $\alpha$  is given by  $-f_l / (\mathbf{F} \mathbf{C}^* \mathbf{e}_l - \mathbf{e}_l)_l = f_l / (1 - (\mathbf{F} \mathbf{C}^*)_l)$ . We state, *without proof*, that this is indeed the flow difference dictated by power flow physics.<sup>14</sup>

Power island, pseudoinverse

<sup>13</sup>The series combination of lines 2, 3 and 4 has a third of the admittance of line 1, so their current must equal a third of the current through line 1.

<sup>14</sup>If we assume the Theorem to be true, one could work backwards from (5.16) to find this result.

Het voorbeeld van een circulair netwerk is te simpel

In the general case of multiple line failures, we essentially apply the above procedure to each failed line, and add the resulting differences. If we were to use this method *iteratively*, by considering the failed lines in some chosen order, we run into the following issue, when more than one line is removed: when removing the second line from the network, we will find a difference flow that sets the second line current to zero. Unfortunately, this difference flow will also change the current of the first line, which is then no longer zero. If we then consider the first line again, we will also affect the second line, et cetera.

To avoid this cat-and-mouse game, we need to find all scaling factors  $\alpha_1, \dots, \alpha_v$  *simultaneously*. By virtue of linearity, the  $v$  conditions imposed by (5.18) form a set of *linear conditions* on  $\alpha = (\alpha_1, \dots, \alpha_v)^T$ .

For each line  $l \in \mathcal{Z}$ , the natural-forced difference is  $\Delta \mathbf{f}^l := \mathbf{F}\mathbf{C}^* \mathbf{e}_l - \mathbf{e}_l$ . When combining all differences for  $l \in [m]$  as columns of a matrix, we find:

$$\begin{pmatrix} | & & | \\ \Delta \mathbf{f}^1 & \dots & \Delta \mathbf{f}^m \\ | & & | \end{pmatrix} = \mathbf{F}\mathbf{C}^* - \mathbf{I} = \mathbf{M}$$

The sub-matrix of differences for  $l \in \mathcal{Z} \subseteq [m]$  is given by:

$$\begin{pmatrix} | & & | \\ \Delta \mathbf{f}^{\mathcal{Z}_1} & \dots & \Delta \mathbf{f}^{\mathcal{Z}_v} \\ | & & | \end{pmatrix} = \mathbf{M}\mathbf{N}$$

Note that  $\mathcal{Z}_1, \dots, \mathcal{Z}_v$  do not need to be ordered.

A linear combination of  $\Delta \mathbf{f}^{\mathcal{Z}_1}, \dots, \Delta \mathbf{f}^{\mathcal{Z}_v}$  with scale factors  $\alpha_1, \dots, \alpha_v$  is given by

$$\Delta \mathbf{f}(\alpha) = \mathbf{M}\mathbf{N}\alpha. \quad (5.19)$$

Condition (5.18) then becomes:

$$\mathbf{N}^* \mathbf{M}\mathbf{N}\alpha = -\mathbf{N}^* \mathbf{f} \quad (5.20)$$

with pseudo-solution

$$\alpha = -(\mathbf{N}^* \mathbf{M}\mathbf{N})^+ \mathbf{N}^* \mathbf{f}. \quad (5.21)$$

Finally, combining (5.19) and (5.21) gives:

$$\Delta \mathbf{f} = -\mathbf{M}\mathbf{N}(\mathbf{N}^* \mathbf{M}\mathbf{N})^+ \mathbf{N}^* \mathbf{f},$$

in agreement with the result. ↩

The proof of Theorem 5.8.1 is given in Ronellenfitsch et al. (2017). This only needs to be adapted to our notation.

## **Part II**

# **Predicting failures in Germany's grid**

## Chapter six

# Methods

The goal of the model described in this thesis can be summarised as follows:

**Given:**

- A real-world *grid structure*
- Hourly *load series*
- Hourly *generation series*

**Predict:**

- ‘*Top 10*’ of lines most likely to fail
- For each risky line: the most likely *cascading line failures*

The model, in particular the use of large deviation statistics to study cascading line failures, was proposed by Nesti et al. (2018a). Following their approach, the model is applied numerically to the SciGRID dataset (Matke et al., 2016). This dataset is an approximation of the transmission network in Germany, including grid structure, generation capacity, hourly load series and hourly renewable generation series.

As discussed in Section ??, transmission lines can fail for a number of reasons, and this model only studies one specific type of failure: *short-term changes in renewable generation*.

Line overloads are, however, the most imminent type of failure in a network, in the sense that grid operators need to continually monitor the *configuration* (distribution among the nodes of power generation) to ensure that no line will overload. This strongly constrains the capability of the transmission network. At any point in time, there could be many configurations that are environmentally (or *economically*) better than the current configuration, but they might lead to a line overload.<sup>1</sup> Turning off functioning

how common are these types of failures?

---

<sup>1</sup>It is for this reason that the Optimal Power Flow problem is computationally difficult solve: it often takes many iterations until a generation distribution is found that does not cause any transmission line to be overloaded.

wind turbines is known as *wind curtailment*, and switching off solar panels is called *solar curtailment*.<sup>2</sup>

In China, as of 2019 the world's largest producer of renewable energy *by a factor of two*, wind curtailment amounted to 16% between 2010 and 2016. (Ye et al., 2018)

ref, wiki

compare to  
european  
consumption

## 6.1 Constructing a complete dataset

European grid operators have detailed datasets that describe the grid structure and state of the transmission network, but these are not (yet) publicly available. We use the work of Brown et al. (2018), which combines open datasets from different sources, to obtain an approximate representation of the German transmission network.

### 6.1.1 Grid structure

The *European Network for Transmission System Operators for Electricity* (ENTSO-E) was established in 2008 to promote the integration between the electricity markets of European member states, and to increase public transparency of these markets. ENTSO-E provides a number of public datasets, including historical hourly load series, international energy flows, and yearly generation series. An up-to-date map can be viewed, containing almost all high-voltage transmission lines in Europe, and lines outside of Europe that are part of the synchronous grid of Continental Europe. Unfortunately, this dataset is not available in a computer-readable format, and only gives the operating voltage and number of parallel circuits of a line.

Luckily, the SciGRID project has assembled an open source dataset of grid structure, using an entirely different source. The OpenStreetMap project is a detailed, open source world map, maintained by a community of mappers. The map is so detailed, in fact, that it not only contains most transmission lines and substations of Europe, it even contains observations of the number of parallel circuits, the number of wires per cable<sup>3</sup>, the frequency<sup>4</sup>, the name of the grid operator, the operating voltage<sup>5</sup>, and the names of the two buses that it connects. From these characteristics, line resistance and inductance can be estimated. The SciGRID dataset has aggregated OpenStreetMap data, and highly simplified the network, resulting in a complete grid structure.

### 6.1.2 Grid state

For our analysis, we need the *hourly* generation series (for each generator at each node), and the hourly load series (aggregated at each node). This data is not publicly available.

<sup>2</sup>Wind turbines can indeed be turned off, by twisting the rotor blades towards 0° pitch and applying the *brakes*. In large turbines, common types are drum brakes (similar to a back-pedalling brake for bikes) and disk brakes. Brakes are especially important during maintenance. Solar panels are switched off using a simple mechanical or electronic switch (a relay). (Denholm et al., 2015)

<sup>3</sup>You can sometimes see that a cable is made up of three wires, with less than a metre of separation between them. This increases the total surface area of the cable with relatively low increase in volume (i.e. cost).

<sup>4</sup>which is always 50 Hz in Europe

<sup>5</sup>This can be deduced from the physical size of the insulators between the cable and the transmission tower (or you could ask the operator).

Yet, previous work (Brown et al., 2018) has shown that these values can be estimated for the German network by combining public sources, in particular:

- SciGRID, which is based on OpenStreetMap data, for the grid structure (as discussed above);
- Data published as part of the German Renewable Energy Sources Act (*Erneuerbare-Energien-Gesetz*), for the location and capacities of solar and wind sources;
- Andresen et al. (2015) provide a world map of hourly solar and wind *potential*, based on weather data and forecasts, for hourly wind and solar series;
- Federal Network Agency of Germany (*Bundesnetzagentur*), for the location and capacities of all other energy sources;
- Global Domestic Product (GDP) and population density of districts (*Landkreise*) of Germany, for load sizes and locations;
- ENTSO-E hourly load series, for hourly load series.

We now have all the data that we need, except for the hourly generation series of *non-stochastic* energy sources. To fill this gap, Brown et al. (2018) use the clever solution of running an Optimal Power Flow (OPF) simulation for each hour, to determine the cheapest generator configuration. The rationale behind this method is that grid operators *use this exact method* to determine the hourly generator configuration. As long as the marginal costs of each generator are realistic, we hope to find a realistic generator configuration this way.

Clearly, the resulting dataset is an *estimation*, and any results that follow from it should be taken with a grain of salt. With this in mind, we proceed with our analysis, not necessarily with the goal of providing accurate operational advice for grid operators, but to demonstrate that the model can be applied to real-world transmission networks. In addition, we hope that this model will provide *qualitative insight* into the complex behaviour of grid failures.

Technical description of resulting dataset

### 6.1.3 PyPSA

context: PSAT for matlab Milano (2005), references 110 and 111 of PSAT manual Milano (2013)

some example graphs

PyPSA:  
Brown et al.  
(2018)

Maybe:  
PyPSA-  
EUR:  
Hörsch et al.  
(2018)



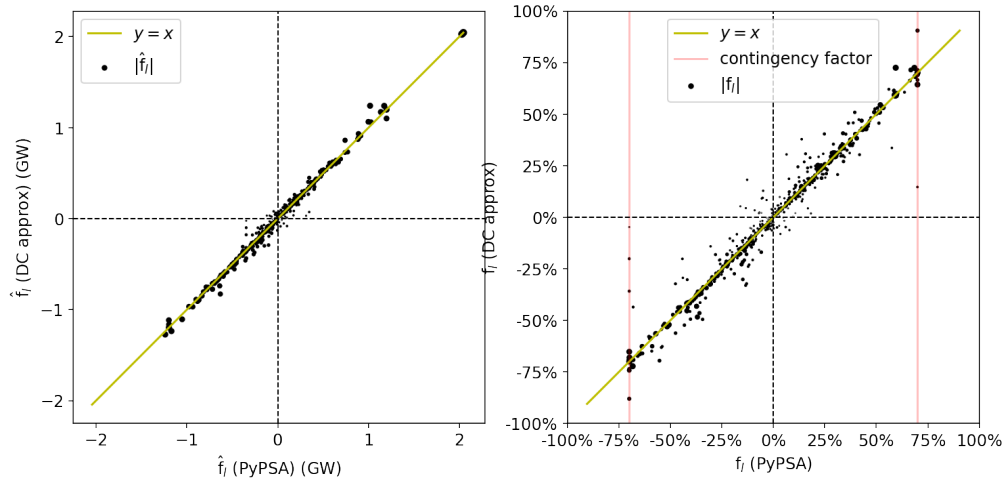


**Figure 6.1:** PLACEHOLDER: Line flow (left) and saturation (right) computed using LPF and (non-linear) PF.

## 6.2 LPF

### 6.2.1 Comparison with PyPSA results

## 6.3 Stochastic power injection

### 6.3.1 Explorative data analysis

### 6.3.2 ARMA model

#### Computing ARMA fits

Following Nesti et al. (2018a), the ARMA models were fitted to the first month of solar and wind generation series using the arima method in R. This produced the desired result for all wind series.

Unfortunately, the arima method failed to fit an ARMA model for 104 of the 489 buses, reflecting the hypothesis that these series are poorly modelled by an ARMA series. To recreate the results of Nesti et al. (2018a), it is crucial that a model can be fitted for *every* bus. Therefore, a modified method is required.

By the default, the arima method operates in two steps. First, a so-called Conditional-Sum-of-Squares (CSS) method is used as initial guess for the ARMA coefficients. Then, the coefficient *likelihood* function is maximised with the Nelder-Mead optimisation method, using the CSS result as initial value.

In our case, the CSS method often finds initial values that are *non-stationary*. A possible reason is that solar generation is exactly zero during nighttime, which lasts for up to 16 consecutive hours.<sup>6</sup> To resolve this issue, we use an optimisation method that works well

define?

<sup>6</sup>In reality, solar generation is never *exactly* zero, even after sunset, because solar panels also receive

without specifying an initial value: it should find the *global* maximum independently. The Simulated Annealing (SANN) algorithm included in R is such a method, and was chosen for this analysis.

With SANN as optimisation method, arima was able to fit solar models for 484 out of 489 buses. For the remaining 5 buses, a second technique is applied: to accommodate for the long periods of zero generation, a small amount of uniform noise is superimposed on the generation series. Initially, the noise magnitude is set to 1% of the solar capacity of the bus. This percentage is increased iteratively, until the modified method is able to fit a solar model. In fact, 1% noise proved sufficient for the remaining 5 buses in January, and no more than 2% noise was needed for any bus in the remaining months.

The modified method described in this section was used to fit solar and wind models to each bus of the network, for each month of 2011. Table 7.1 lists the number of buses that can be analysed using the default and modified methods, showing the poor performance of the default for solar series, especially during the months of summer.

Nesti et al. (2018a) do not mention such problems (nor techniques to solve them). Because the same dataset, processing, programming language and method was used in this analysis, it is likely that they have also encountered and solved these problems, possibly in the same manner.

Belisle 1992,  
zie optim  
docs

discuss other possible techniques: warm start, intercept

## Runtime

The default implementation has an estimated (single-core) runtime of 101 hours (4.2 days) when all 12 months are analysed, although only 78% of fits are successful using this method.

The modified version is able to fit all generation series successfully. The use of this more computationally expensive method increases the runtime to an estimated 224 hours (9.4 days). Because of the long runtime, fits were computed in parallel on a 40-core machine<sup>7</sup>, provided by the IT department of the Radboud University.<sup>8</sup> This reduced the total runtime down to 7 hours. The results are publicly available at the GitHub repository.

### 6.3.3 Stochastic line flows

## 6.4 Line failures

## 6.5 Cascading line failures

ambient light. This is not included in the (artificial) dataset.

<sup>7</sup>Specifications: two *Intel Xeon E5 2630L v4* 10-core processors @2GHz with hyperthreading; 64GB RAM. CPU time was used as estimate for single-core runtime.

<sup>8</sup>Thank you!

## Chapter seven

# Results

In this final chapter, we

### 7.1 SciGRID data

The SciGRID dataset needs to be translated into the our model, as it contains more information than we need, not yet in the desired format.

#### 7.1.1 Properties

*(A more detailed analysis of dataset properties is available on the GitHub repository.)*

Before any processing, we find that the SciGRID network (obtained from PyPSA example code, the exact dataset used by Nesti et al. (2018a)) contains 585 buses, 1423 generators (of all sources) and 489 loads. It also contains 38 storage units (all are pumped hydro-electric), but these were excluded from our analysis.<sup>1</sup> There are 852 transmission lines in the dataset, at possible voltage levels 220 kV and 380 kV, and there are 96 transformers (between these two voltages). Transmission lines have per-kilometre estimates for admittance, from which the total admittance can be deduced.

#### Voltages

In our model, we *normalise* the grid voltage. To do so, we multiply all line admittances by the *square* of their operating voltages, after which all voltages can be assumed to be 1, and a unit of current is proportional to a unit of transmitted power. Of the 585 buses, 192 are part of one of the 96 *voltage pairs*: these are two buses at the same location, with the same name (except for the voltage suffix), connected via a transformer. By merging these pairs, we find 489 geographically unique buses, at normalised voltage. From now on, we will refer to these (possibly merged) buses as the buses of the network:  $n = 489$ ,  $\mathcal{N} = [489]$ .

---

<sup>1</sup>More specifically, they were used in solving the OPF problem, but their initial charge was set to zero.

## Loads

There is exactly 1 load connected to each bus. In reality, there are of course thousands of loads connected to a bus, but the load in the dataset is the *aggregated* load at that bus. We have hourly time series (i.e. amount of MW being consumed) for each node in the year 2011, which only includes active power consumption.

## Generators

Generators are connected to the geographically closest bus, and there is at most one generator per bus of each type.<sup>2</sup> This means that generation is *aggregated*: multiple generators of the same type are combined into one. There are 489 solar generators, 488 onshore wind generators and 5 offshore wind generators. Offshore wind generators are connected to buses at the north coast of Germany. This means that every bus houses stochastic generation. Their geographic distribution is shown in Figure 7.2.

## Lines

Line voltages and admittances are normalised as described above. For each line, we have the names of the two original buses that it connects, which can easily be converted to the new bus collection.

During the study of cascading failures, we found that the network contains *parallel lines*: lines that connect the same pairs of buses. In some cases, there are up to four different lines that are all parallel. When examining these cases on OpenStreetMap, we find that there are indeed parallel lines in the physical network. This is reflected by the *lengths* of parallel lines, as given by SciGRID: these are not the great-circle distances between buses, but rather the distance measured along the line (which makes some turns and bends).

Because our model only holds for *digraphs*, which cannot have parallel lines, we *combine* parallel lines, by summing their (voltage normalised) admittances, and summing their thresholds.<sup>3</sup> Nesti et al. (2018a) do not mention this anomaly, and use the original set of lines. For comparison, we computed some results for both versions of the network, and found the results to be somewhat similar, in general. Because we did not consider the case of parallel lines in our model, combining parallel lines in the dataset seems like the *correct* choice.

Of the 852 original lines, there are 705 unique links between original buses before normalising voltages, and there are 695 unique links between buses. There are never two parallel lines with opposite orientation. These 695 lines were used in our model, and will be referred to as simply the *lines* of the network:  $m = 695$ .

---

<sup>2</sup>In order of installed capacity: *Wind Onshore* (37 GW), *Solar* (37 GW), *Hard Coal* (25 GW), *Gas* (24 GW), *Brown Coal* (21 GW), *Nuclear* (12 GW), *Run of River* (4 GW), *Other* (3 GW), *Wind Offshore* (3 GW), *Oil* (2.7 GW), *Waste* (1.6 GW), *Storage Hydro* (1.4 GW), *Multiple* (0.15 GW) and *Geothermal* (32 MW).

<sup>3</sup>The results regarding the kernel of FRT, and the Optimised method for analysis cascading failures, break down without this property.

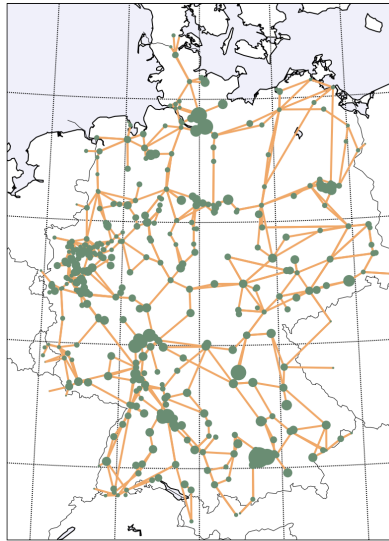


**Figure 7.1:** PLACEHOLDER: The load distribution of Germany at ???.

## 7.2 Bus covariance

## 7.3 Line covariance

By incorporating bus covariances in our model (which result from correlated weather), we hope to find new structure in the line covariances. To assess the effect of estimating bus covariances, we compare three possible bus covariance matrices:

1. *The identity matrix*: all bus injections are independently Gaussian distributed with the same variance. (They are almost IID, but their means differ.)
2. *The diagonal of estimated variances*: all bus injections are independently Gaussian distributed, but their variances and means differ.
3. *The estimated covariances*: the vector of bus injections is (multivariate) Gaussian distributed. All bus injections are, in general, dependent on each other, and their variances and means differ.

We expect the covariance of a random pair of lines to be relatively low, when their physical separation (measured either in kilometres or in graph distance) is high. Because weather is correlated, even at high distance, using the bus full covariance might result in higher covariances between lines with high separation. (This was concluded by Nesti et al. (2018a).)

Using a different bus covariance matrix will likely result in an overall increase or decrease of line covariances. Note, however, that the line covariance matrix is scaled by an arbitrary factor  $\epsilon$ , so any overall change in covariance has no significance in the model.

Compare three bus covariance

Maar als je normaliseert op variantie?

asdf

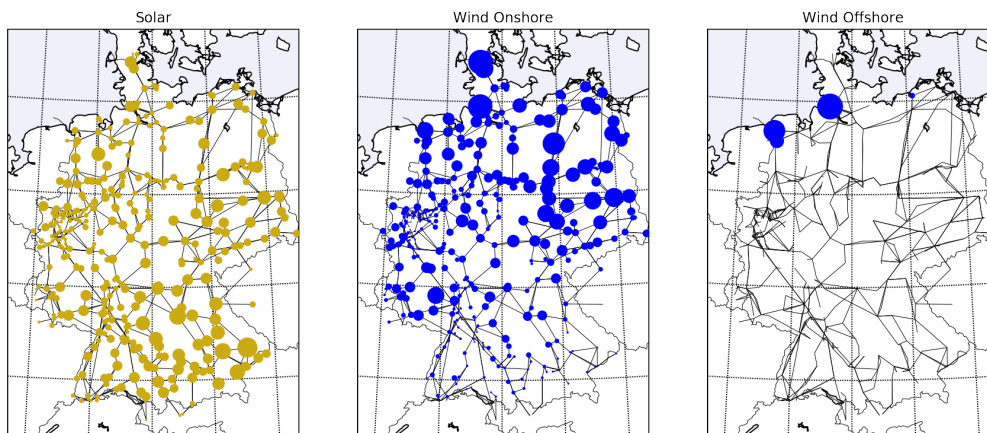


**Figure 7.2:** PLACEHOLDER: Solar, wind onshore, wind offshore generation at ?? in Germany.

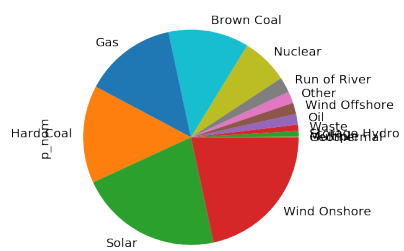


**Figure 7.3:** PLACEHOLDER: Generation capacity technology shares in Germany in 2011.

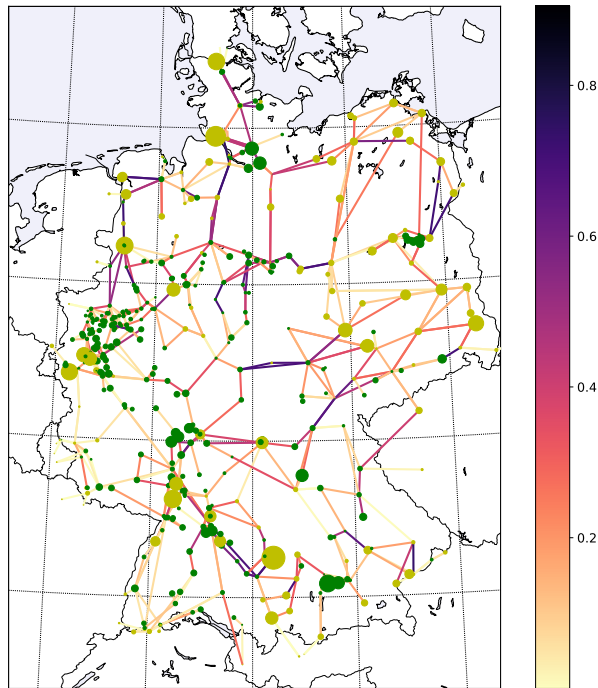


**Figure 7.4:** Nominal line flow during 11:00-12:00, as fraction of line capacity. Node size represents net power injection. When generation exceeds load, the injection is positive (yellow), otherwise negative (green). *Compare with Figure 1a of Nesti et al. (2018a).*

Plotjes van  
kansen zoals  
in

	SOLAR				WIND			
	<i>default</i>	<i>modified</i>	1%	2%	<i>default</i>	<i>modified</i>	1%	2%
Jan	385	<b>484</b>	<b>5</b>	<b>0</b>	<b>488</b>	488	<b>0</b>	<b>0</b>
Feb	364	<b>485</b>	<b>4</b>	<b>0</b>	<b>487</b>	487	<b>0</b>	<b>1</b>
Mar	334	<b>475</b>	<b>14</b>	<b>0</b>	<b>487</b>	487	<b>1</b>	<b>0</b>
Apr	211	<b>477</b>	<b>11</b>	<b>1</b>	<b>488</b>	488	<b>0</b>	<b>0</b>
May	189	<b>473</b>	<b>16</b>	<b>0</b>	<b>467</b>	467	<b>21</b>	<b>0</b>
Jun	255	<b>481</b>	<b>8</b>	<b>0</b>	<b>480</b>	480	<b>8</b>	<b>0</b>
Jul	292	<b>485</b>	<b>4</b>	<b>0</b>	<b>488</b>	488	<b>0</b>	<b>0</b>
Aug	179	<b>478</b>	<b>10</b>	<b>1</b>	<b>488</b>	488	<b>0</b>	<b>0</b>
Sep	259	<b>472</b>	<b>16</b>	<b>1</b>	<b>487</b>	487	<b>1</b>	<b>0</b>
Oct	263	<b>480</b>	<b>9</b>	<b>0</b>	<b>488</b>	488	<b>0</b>	<b>0</b>
Nov	290	<b>472</b>	<b>17</b>	<b>0</b>	<b>486</b>	486	<b>2</b>	<b>0</b>
Dec	317	<b>482</b>	<b>7</b>	<b>0</b>	<b>486</b>	486	<b>2</b>	<b>0</b>

**Table 7.1:** Number of buses (out of 489 solar, 488 wind) for which the ARMA model could be fitted using either the *default* implementation of arima in R, or the *modified* version (described in 6.3.2).

When even the modified method yielded no results, uniform noise was added to the series before fitting. Noise magnitude was set to 1% of generation capacity, or 2% when needed.

Figures in **bold** indicate which results are used.



$l$	$\mathbb{P}[ f_l  \geq 1]$	$I_l$
361	3.45 %	1.65
516	2.91 %	1.79
586	2.75 %	1.84
587	2.73 %	1.85
803	2.02 %	2.10
670	1.21 %	2.54
19	1.13 %	2.60
302	1.08 %	2.64
48	1.03 %	2.68
554	0.974%	2.73
488	0.971%	2.73
809	0.824%	2.88
28	0.748%	2.96
810	0.728%	2.98
29	0.396%	3.53
27	0.355%	3.62
389	0.247%	3.95
390	0.245%	3.96
486	0.235%	4.00
249	0.056%	5.30

**Table 7.2:** TODO

# Bibliography

- Andresen, G. B., A. A. Søndergaard, and M. Greiner  
2015. Validation of Danish wind time series from a new global renewable energy atlas for energy system analysis. *Energy*.
- Brown, T., J. Hörsch, and D. Schlachtberger  
2018. PyPSA: Python for Power System Analysis. *Journal of Open Research Software*, 6(1):4.
- Chertkov, M., M. Stepanov, F. Pan, and R. Baldick  
2011. Exact and efficient algorithm to discover extreme stochastic events in wind generation over transmission Power Grids. In *IEEE Conference on Decision and Control and European Control Conference*, Pp. 2174–2180. IEEE.
- Denholm, P., M. O’connell, G. Brinkman, and J. Jorgenson  
2015. Overgeneration from Solar Energy in California: A Field Guide to the Duck Chart. Technical report, National Renewable Energy Laboratory.
- Garling, D. J. H.  
2014. *A course in mathematical analysis. Volume III, Complex analysis, measure and integration*. Cambridge: Cambridge University Press.
- Hörsch, J., F. Hofmann, D. Schlachtberger, and T. Brown  
2018. PyPSA-Eur: An open optimisation model of the European transmission system. *Energy Strategy Reviews*, 22:207–215.
- Kirtley, J. L.  
2010. *Electric power principles: sources, conversion, distribution, and use*. John Wiley & Sons, Ltd.
- Matke, C., W. Medjroubi, and D. Kleinhans  
2016. SciGRID - An Open Source Reference Model for the European Transmission Network (v0.2).
- Matoušek, J. and B. Gärtner  
2007. *Understanding and using linear programming*. Springer.
- Milano, F.  
2005. An Open Source Power System Analysis Toolbox. *IEEE Transactions on Power Systems*, 20(3):1199–1206.

- Milano, F.  
2013. Power System Analysis Toolbox. Documentation for PSAT version 2.0.0.
- Nesti, T., A. Zocca, and B. Zwart  
2018a. Emergent Failures and Cascades in Power Grids: A Statistical Physics Perspective. *Physical Review Letters*, 120(25):258301.
- Nesti, T., A. Zocca, and B. Zwart  
2018b. Supplemental Material for: Emergent failures and cascades in power grids: a statistical physics perspective. Technical report.
- Overbye, T., Xu Cheng, and Yan Sun  
2004. A comparison of the AC and DC power flow models for LMP calculations. *37th Annual Hawaii International Conference on System Sciences, 2004. Proceedings of the*, 00(C):9 pp.
- Pestman, W. R.  
1998. *Mathematical statistics - an introduction*. Nijmegen: Walter de Gruyter.
- Purchala, K., L. Meeus, D. Van Dommelen, and R. Belmans  
2005. Usefulness of DC power flow for active power flow analysis. *IEEE Power Engineering Society General Meeting, 2005*, Pp. 2457–2462.
- Ronellenfitsch, H., D. Manik, J. Hörsch, T. Brown, and D. Witthaut  
2017. Dual Theory of Transmission Line Outages. *IEEE Transactions on Power Systems*, 32(5):4060–4068.
- Slepian, P.  
1968. *Mathematical Foundations of Network Analysis*, volume 16 of *Springer Tracts in Natural Philosophy*. Berlin, Heidelberg: Springer Berlin Heidelberg.
- Touchette, H.  
2009. The large deviation approach to statistical mechanics. *Physics Reports*, 478(1-3):1–69.
- von Meier, A.  
2006. *Electric Power Systems*. Hoboken, NJ, USA: John Wiley & Sons, Inc.
- Ye, Q., L. Jiaqi, and Z. Mengye  
2018. Wind Curtailment in China and Lessons from the United States. Technical report, Brookings.

# Index

- AC generator, 20
- admittance, 30
  - matrix, 30
  - vector, 30
- cascading failures, 30
- circuit breaker, 22
- configuration, 26, 53
  - admissible, 26
  - balanced, 26
  - possible, 26
- curtailment
  - solar, 54
  - wind, 54
- DC approximation
  - state, 39
  - structure, 39
- distribution
  - elementary Gaussian, 6
  - elementary normal, 6
  - Gaussian, 6
  - normal, 6
  - standardised normal, 8
- electric inertia, 20
- emergent failure, 8
- energy storage, 20
- flat profile, 39
- flow, 13
- Flow Response Transformation, 13
- generation capacity, 25
- generator, 20
- graph
  - directed, 12
- grid
  - state, 32
  - structure, 30
- induced injection, 13
- injection, 13
- inverter, 20
- isolated node, 13
- KCL equality, 36
- KVL-Ohm equality, 36
- line capacity, 22
- line drop, 23
- line failure, 22
- line flow
  - normalised, 44
- line threshold, 44
- Linear Optimum Power Flow (LOPF), 27
- Linearised Power Flow (LPF), 27
- load following, 26
- load profile, 26
- load profiling, 29
- loop flow, 16
- marginal cost, 25
- net injection, 14
- network
  - $n$ -loop, 31
  - two-node, 31
- nodal susceptance matrix, 37
- node flow equation, 36
  - approximate, 39
- normalised profile, 39
- operating voltage, 39
- Optimum Power Flow (OPF), 27
- overload, 22

pillar, 7  
plane, 7  
polyhedron, 8  
power angle, 37  
power injector, 33  
power island, 29  
ready to deploy, 26  
slack bus, 26  
stability limit, 37  
thermal limit, 22  
valid, 36  
    DC, 39